การปรับปรุงความว่องไวของตัวเร่งปฏิกิริยาทางไฟฟ้าเคมีที่ไม่เป็นไปตามกฎของฟาราเดย์ของการ
ออกซิเดชันโพรเพนที่ฟิล์มบางบนอะลูมินา

นางสาวพัทธมน ลิ้มศรีมงคลชัย

วิทยานิพนธ์นี้เป็นส่วนหนึ่งของการศึกษาตามหลักสูตรปริญญาวิศวกรรมศาสตรมหาบัณฑิต
สาขาวิชาวิศวกรรมเคมี ภาควิชาวิศวกรรมเคมี
คณะวิศวกรรมศาสตร์ จุฬาลงกรณ์มหาวิทยาลัย
ปีการศึกษา 2559
ลิขสิทธิ์ของจุฬาลงกรณ์มหาวิทยาลัย

NON-FARADAIC ELECTROCHEMICAL MODIFICATION OF CATALYTIC ACTIVITY
(NEMCA) OF PROPANE OXIDATION AT THIN-FILM CELL ON ALUMINA

Miss Pattamon Limsrimongkonchai

A Thesis Submitted in Partial Fulfillment of the Requirements

for the Degree of Master of Engineering Program in Chemical Engineering

Department of Chemical Engineering

Faculty of Engineering

Chulalongkorn University

Academic Year 2016

Thesis Title	NON-FARADAIC ELECTROCHEMICAL MODIFICATION OF CATALYTIC ACTIVITY (NEMCA) OF PROPANE OXIDATION AT THIN-FILM CELL ON ALUMINA
By	Miss Pattamon Limsrimongkonchai
Field of Study	Chemical Engineering
Thesis Advisor	Palang Bumroongsakulsawat, Ph.D.

Accepted by the Faculty of Engineering, Chulalongkorn University in Partial Fulfillment of the Requirements for the Master's Degree

....Dean of the Faculty of Engineering

(Associate Professor Supot Teachavorasinskun, Ph.D.)

THESIS COMMITTEE

....Chairman

(Professor Suttichai Assabumrungrat, Ph.D.)

....Thesis Advisor

(Palang Bumroongsakulsawat, Ph.D.)

....Examiner

(Professor Bunjerd Jongsomjit, Ph.D.)

....External Examiner

(Assistant Professor Worapon Kiatkittipong, Ph.D.)

พัทธมน ลิ้มศรีมงคลชัย : การปรับปรุงความว่องไวของตัวเร่งปฏิกิริยาทางไฟฟ้าเคมีที่ไม่
เป็นไปตามกฎของฟาราเดย์ของการออกซิเดชันโพรเพนที่ฟิล์มบางบนอะลูมินา (NON-
FARADAIC ELECTROCHEMICAL MODIFICATION OF CATALYTIC ACTIVITY (NEMCA)
OF PROPANE OXIDATION AT THIN-FILM CELL ON ALUMINA) อ.ที่ปรึกษา
วิทยานิพนธ์หลัก: ดร. พลัง บำรุงสกุลสวัสดิ์, 79 หน้า.

งานวิจัยนี้ศึกษาเกี่ยวกับการปรับปรุงความว่องไวของตัวเร่งปฏิกิริยาทางไฟฟ้าเคมีที่ไม่
เป็นไปตามกฎของฟาราเดย์ (ปรากฏการณ์เนมคา) สำหรับโพรเพนออกซิเดชัน ซึ่งเป็นปรากฏการณ์
ในการปรับปรุงระบบเครื่องฟอกไอเสียเชิงเร่งปฏิกิริยา โดยสารประกอบเซอร์โคเนียเจือด้วยอิตเทรีย
หรือวายเอสแซด เป็นอิเล็กโทรไลต์ที่มีสมบัติเป็นตัวนำไอออน นำมาทำเป็นชั้นฟิล์มบางบนตัว
รองรับอะลูมินา โดยใช้เทคนิคการสปัตเตอริงในระบบสุญญากาศ โดยศึกษาปฏิกิริยาภายใต้สภาวะ
อุณหภูมิที่ 200-500 องศาเซลเซียส ในสภาวะวงจรแบบเปิด(ไม่มีการให้กระแสไฟฟ้าหรือศักย์ไฟฟ้า)
และวงจรแบบปิด(มีการให้กระแสไฟฟ้าหรือศักย์ไฟฟ้า) ด้วยรูปแบบของเซลล์ระหว่างวิธีไร้สายและวิธี
ดั้งเดิม ซึ่งวิธีแบบไร้สายจะได้อัตราการเกิดแก๊สคาร์บอนไดออกไซด์สูงสุด เท่ากับ 1.98×10^{-8} โมล
ต่อวินาที ด้วยการสปัตเตอริงที่กำลัง 400 วัตต์ เป็นเวลา 4 ชั่วโมง ในขณะที่วิธีแบบดั้งเดิม ที่อุณหภูมิ
500 องศาเซลเซียส ปรากฏการณ์เนมคาจะแสดงพฤติกรรมชนิดอิเล็กโตรโฟบิค (อัตราการ
เกิดปฏิกิริยาจะเพิ่มมากขึ้นเมื่อมีการให้ศักย์ไฟฟ้าที่เป็นบวก) โดยในการเพิ่มและลดความต่างศักย์
อัตราการเกิดปฏิกิริยาสามารถแสดงการผันกลับได้ที่อุณหภูมิ 400 องศาเซลเซียส สำหรับการสปัตเต
อริงที่ 4 ชั่วโมง และที่อุณหภูมิ 200 องศาเซลเซียสสำหรับการสปัตเตอริงที่ 8 ชั่วโมง ทั้งนี้เทคนิค
การพิมพ์สกรีนสำหรับการทำชั้นฟิล์มบางของวายเอสแซดได้นำมาศึกษาเช่นเดียวกัน โดยวิธีแบบไร้
สายให้ค่าอัตราส่วนระหว่างการเกิดปฏิกิริยาที่วงจรแบบปิดต่อที่วงจรแบบเปิด มีค่าสูงสุดเท่ากับ 2 ที่
ปริมาณความเข้มข้นวายเอสแซดที่ 60 เปอร์เซ็นต์โดยน้ำหนัก และวิธีแบบดั้งเดิมให้ค่าอัตราส่วนสูงสุด
เท่ากับ 1.31

ภาควิชา	วิศวกรรมเคมี	ลายมือชื่อนิสิต	
สาขาวิชา	วิศวกรรมเคมี	ลายมือชื่อ อ.ที่ปรึกษาหลัก	
ปีการศึกษา	2559		

5870201421 : MAJOR CHEMICAL ENGINEERING

KEYWORDS: PROPANE OXIDATION, YSZ, THINFILM, NEMCA

PATTAMON LIMSRIMONGKONCHAI: NON-FARADAIC ELECTROCHEMICAL MODIFICATION OF CATALYTIC ACTIVITY (NEMCA) OF PROPANE OXIDATION AT THIN-FILM CELL ON ALUMINA. ADVISOR: PALANG BUMROONGSAKULSAWAT, Ph.D., 79 pp.

Non-faradaic electrochemical modification of catalytic activity (NEMCA) of propane oxidation has been studied. It is a potential phenomenon that could become a breakthrough in improvements on catalytic converters. Yttria-stabilized zirconia (YSZ, Y_2O_3:ZrO_2) ionic conductors, was deposited on alumina substrates by sputtering technique carried out in vacuum in the form of a thin film deposited on a cheaper alumina support. NEMCA of propane oxidation was studied under a stoichiometric ratio of propane to oxygen at 200-500 °C in both open-circuit (i.e., with no current passing through the electrolyte) and closed-circuit conditions with wired configuration cell between wireless and conventional methods. The highest catalytic CO_2 production rate is 1.98 x 10^{-8} mol/s by wireless method operated by sputtering at 400 W for 4 h while in case of conventional method, at 500 °C with YSZ thin film cells, the reaction rate exhibited the electrophobic type of NEMCA (i.e., the promoting effect at positive potentials) at closed-circuit condition. However, reversibility of reaction rates was observed during forward and reverse potential scans at 400°C for sputtering time 4 h and 200 °C for sputtering time 8 h. Moreover, screen-printing technique was also fabricated YSZ thin film on alumina. By wireless method, the maximum rate enhancement ratios was 2 times at 60wt% YSZ ink and by conventional method, the maximum rate enhancement ratios was 1.31 times.

Department:	Chemical Engineering	Student's Signature	....
Field of Study:	Chemical Engineering	Advisor's Signature	....
Academic Year:	2016		

ACKNOWLEDGEMENTS

CONTENTS

TABLES OF CONTENTS

FIGURES OF CONTENTS

CHAPTER I

INTRODUCTION

1.1 Background

The catalytic oxidation of hydrocarbons is a dominant industrial route to the production of many important chemicals[1]. The catalytic combustion of hydrocarbons especially propane, is an important technology both for emission control and for energy production in the industrial sectors.

The electrochemical promotion of catalysis (EPOC) or non-faradaic electrochemical modification of catalytic activity (NEMCA) has been studied extensively for more than 15 years almost exclusively in research laboratories but there is also a strong industrial interest and involvement aiming to its commercialization. NEMCA is an innovative concept which can be used to improve the catalytic activity. It is based on the control of the work function due to the electrochemical pumping of ions (O^{2-}) by an applied potential between a solid electrolyte (Y_2O_3 -stabilized ZrO_2, YSZ) and the surface of a porous catalyst (Pt)[2, 3]. Platinum is the catalyst most widely used for the combustion of propane and it has been studied by a large number of investigators [4-7]. NEMCA has been investigated in the field of catalytic and environmental protection. It is a potential phenomenon that could become a breakthrough in improvements on catalytic converters.

The electrochemical promotion effect refers to the very pronounced and reversible changes in the catalytic properties of conductive catalysts deposited on solid electrolytes caused by application of small electrical currents or potentials. Yttria-stabilized zirconia (YSZ) is commonly used as oxygen ion-conducting electrolyte material[8, 9]. However, this material is much more expensive than common catalyst supports such as alumina. In order to reducing the cost of YSZ, electrolyte thin films over common catalyst supports such as alumina were investigated.

It is therefore envisaged that in a commercially feasible NEMCA-enhanced catalytic converter be incorporated only a sufficient amount of YSZ in the form of a thin film deposited on a cheaper rigid support. A catalyst and the necessary electrodes are then deposited on the thin YSZ film. Techniques that have been used to deposit YSZ include chemical vapor deposition[10, 11], pulsed laser deposition[12-15], radio frequency(RF) sputtering[16, 17], ion beam sputtering[18], molecular beam epitaxy [19] and sol-gel deposition[20]. All of these techniques produced fully oxidized YSZ.

In this work, propane oxidation at Pt-YSZ was studied. YSZ was deposited on alumina disks by RF magnetron sputtering. The catalyst potential was measured between the working electrode (Pt) and the reference electrode (Au). Gold was selected because of its negligible catalytic activity in propane oxidation, as verified through blank experiments under our experimental conditions. Under open circuit, the cell operated as a regular catalytic reactor and the kinetics of the reaction were studied in conjunction with measurements of the cell potential. Under closed circuit, the effect of oxygen ion pumping on the catalytic activity of Pt was investigated. Both, open- and closed circuit results obtained with this catalyst electrode is evaluated in order to achieve optimal catalytic performances.

1.2 Research objectives

1.2.1 To fabricate YSZ thin film on alumina substrate.

1.2.2 To study NEMCA effect at thin film cell and compare the dependence of propane oxidation rates on applied potentials and temperature at Pt-YSZ.

1.3 Research scopes

1.3.1 Effects of wired configuration cell between wireless and conventional methods.

1.3.2 Effects of potential differences 0 volts up to 30 volts on reaction rates.

1.3.3 Effects of the temperature with 200-500 °C on reaction rates.

1.3.4 Fixed feed compositions at 3% propane, 10% oxygen balance helium.

1.3.5 Platinum and gold used as working and counter electrode, respectively.

CHAPTER II

THEORY & LITERATURE REVIEW

2.1 Theory

2.1.1 Non-Faradaic Electrochemical Modification of Catalytic Activity (NEMCA)

Non-Faradaic Electrochemical Modification of Catalytic Activity (NEMCA), or Electrochemical Promotion Of Catalysis (EPOC) is due to an electrochemically induced and controlled reversible spillover of ions from solid electrolyte onto the catalyst surface[1]. This phenomenon induces variation in the catalyst work function upon current or potential application and also improves catalytic converter function. NEMCA has been observed in O^{2-}, Na^+, K^+, Pb^{2+} and H^+ conductors [1, 21, 22] as solid electrolytes and used in solid electrolyte cell-reactors. For example the reaction under study is the oxidation of propane:

$$C_3H_8 + 5\,O_2 \longrightarrow 3\,CO_2 + 4\,H_2O \qquad (1)$$
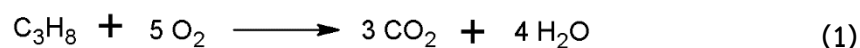
The cell consists of a dense solid electrolyte membrane and two electrodes, deposited on the two sides of the electrolyte. The circuit is open, gaseous propane is fed together with oxygen, the cell is operated as a regular catalytic reactor and the kinetics of the reaction were studied in conjunction with measurement of the cell potential. When the circuit is closed, a constant voltage is applied. An electrochemical oxygen of the cell was "pump" on the catalytic activity of electrode as shown in Figure 2.1
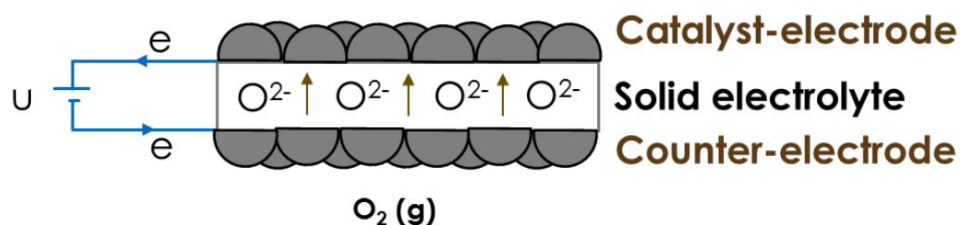
Figure 2.1 An O^{2-} conducting solid electrolyte [23]

The parameters that are commonly used to quantify the magnitude of NEMCA effects [24] are:

1) The rate enhancement ratio, ρ, defined by:

$$\rho = r/r_0 \tag{2}$$

where r is the electropromoted catalytic rate

r_0 is the open-circuit rate, i.e. non-promoted catalytic rate

2) The apparent Faradaic efficiency, Λ, defined by :

$$\Lambda = (r - r_0)/(I/nF) \tag{3}$$

where I is the applied current,

n is the charge of the promotion ion

F is Faraday's constant

2.1.2 Sputtering

Sputter deposition is a physical vapor deposition (PVD) method by sputtering is a process which particles are ejected from a solid target material due to bombardment of the target by energetic particles onto a substrate e.g. alumina. In sputtering, the target material and the substrate are placed in a vacuum chamber. A plasma is originated by ionizing a sputtering gas (generally a chemically inert, heavy gas like argon) and sputtering deposition usually uses an argon which is the most commonly employed process gas for sputter deposition processes and argon is a noble gas will not react with the target material and is relatively inexpensive (compared with the other noble gases (Krypton and Xenon). Sputtered atoms ejected from the target have a wide energy distribution deposit as a film on substrate (Figure 2.2).

The Oerlikon Leybold Univex 350 RF sputtering system is a tool used for the deposition of both metal and dielectric films using two magnetron sputter guns. A process wherein an argon plasma is generated, and charged argon ions are accelerated towards the target to kinetically knock target material off in random directions towards the substrate. The rotation of the target and the angled sputter guns allows for good film thickness uniformity across a full 4" wafer.
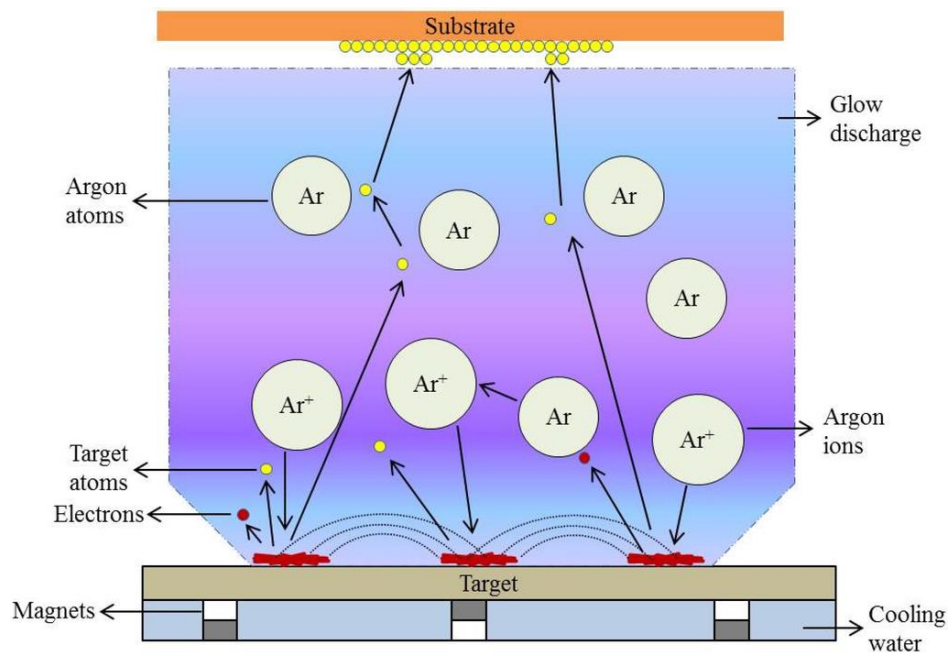
Figure 2.2 Sputtering process

RF or Radio Frequency Sputtering is technique implicated in the electrical potential of the current in the vacuum environment at radio frequencies to avoid a charge up types of sputtering target materials, which over time can result in arcing into the plasma that spews droplets appointing quality control issues on the thin films. RF Sputtering offers several advantages. A plasma throughout chamber at a lower pressure depending on gas sputter. The result is fewer ionized gas collisions equaling more efficient line-of-site deposition of the coating material.

While RF Sputtering can be used for most types of thin film deposition, it has become choice of the thin film deposition technique for many types of dielectric coatings - insulating coatings which are non-conducting can take on a polarized charge. RF Sputtering is important for the semiconductor industry producing highly insulating oxide films between the thin film layers of microchip circuitry including aluminum oxide, silicon oxide and tantalum oxide.

2.1.3 Platinum

The most common use of platinum is as a catalyst in chemical reactions. It is most important application in automobiles as a catalytic converter, which allows the complete combustion at low concentrations of unburned hydrocarbons from the exhaust into carbon dioxide and water vapor. At present 98 tones were used for vehicle emissions control devices. Platinum is the standard catalyst for many oxidation and reduction reactions in both acidic and basic electrolytes and would be an ideal candidate for process feasibility studies.

The role of platinum in catalytic converters is oxidize carbon monoxide (CO) and hydrocarbons, so is often the metal choice for diesel applications. For powered vehicles platinum and palladium can be equally effective. However platinum has several advantages including high melting point,   interactions with poisons (such as sulfur   compounds) are restricted to the metal surface and also efficiently recycled.

In a catalytic converter, the metal is formed of nanoparticles, which are dispersed over the whole surface of a highly porous support materials. As the catalyst temperature increase, the particles start to become mobile and can coalesce. Moreover, metals such as copper and silver have a high affinity for sulfur molecules, with react to form compounds such as metal sulfates or sulfides. As this catalyst, there will be progressively less metal available useful for reactions to take place. However, Platinum is different because it tends not to become totally or irreversibly poisoned, i.e. sulfur molecules inhibit rather than poison platinum based catalysts.

Table 2.1 The physical and chemical properties of Platinum.

Properties	Value
Symbol	Pt
Atomic Number	78
Atomic Weight	195.09
Density	21.45 gm/cc
Melting Point	1772 °C
Boiling Point	3827 °C
Thermal Conductivity	0.716 W/cm/K @ 298.2 K

The working electrode indicate the most important component of an electrochemical cell. It is at the interface between the working electrode and the solution that electron transfers of greatest interest occur. The commonly used working electrode materials are platinum, gold, carbon, and mercury. Among these, platinum is likely the favorite, showing good electrochemical, inertness and ease of fabrication into many forms. The disadvantage for use of platinum, other than its high cost. Lizarraga et al.,[25] present the variation of the catalytic activity for the propane oxidation corresponding to the sputtered and paste-Pt films. The values of sputtered-Pt films was 50%, which higher than for Pt-paste films. The low values obtained for Pt-paste films was due to the high OCV conversion.

Table 2.2 NEMCA parameters obtained on the Pt- sputter and the Pt-paste electrochemical catalysts[25].

Electrocatalyst	Anodic current	Λ	ρ
Pt-sputter films	500	153	22.4
	100	361	11.2
	50	480	7.8
Pt-paste films	500	109	1.4
	100	274	1.2

2.1.4 Gold

Gold electrodes have similarly with platinum, but have limited usefulness in the positive potential range caused the oxidation of its surface. Both platinum and gold films are deposited by vacuum deposition, sputtering and screen-printing techniques. Adhesion layers are often used to produce well-adhering films.

Gold ink is an excellent conductor of current, which makes it a very useful contact paste. This gold ink is also screen printable which makes it useful for fabricating electrochemical devices. This is a great ink for making electrical connections for electrochemical testing of fuel cells, ceramic substrates, electrochemical materials, and metals, and for making a gas tight seal. The physical and chemical properties of

gold and advantages and limitations of platinum and gold as shown in Table 2.3 and Table 2.4 , respectively.

Table 2.3 The physical and chemical properties of gold.

Properties	Value
Symbol	Au
Atomic Number	79
Atomic Weight	196.97
Density	21.45 gm/cc
Melting Point	1064 $^{\circ}$C
Boiling Point	3827 $^{\circ}$C
Thermal Conductivity	0.716 W/cm/K @ 298.2 K

Table 2.4 Advantages and limitations of platinum and gold.

Materials	Advantages	Limitations
Pt	Available wire, flat plate & tube large range of sizes Pt-Rh alloy for rigidity	Low hydrogen overvoltage so cathodic potential range limited and expensive
Au	Configurations same as Pt larger cathodic potential range	Larger cathodic potential range anodic window limited by surface oxidation expensive

2.1.5 Yttria-stabilized zirconia (YSZ)

Yttria stabilized zirconia (YSZ), is an oxygen ion conductor for catalytic applications. This ceramic material be compound with several functionalities such as good thermal stability, selective bulk oxygen mobility and high surface oxygen vacancy concentration. These properties have been first exploited, utilizing YSZ as dense membranes, in applications of solid oxide fuel cells and electrochemical promotion of catalysis. More recently, YSZ, as nanopowders, has also been considered as a promising support for metallic nanoparticles [26].

The mostly used composition of YSZ contains 8 mol% yttria, which stabilizes the cubic phase of zirconia [27, 28]. Zirconia (ZrO_2) is a thermal insulator with high thermodynamic and chemical stability. Doping zirconia with yttria (Y_2O_3) replaces Zr^{4+} with Y^{3+} as shown in Figure 2.3.
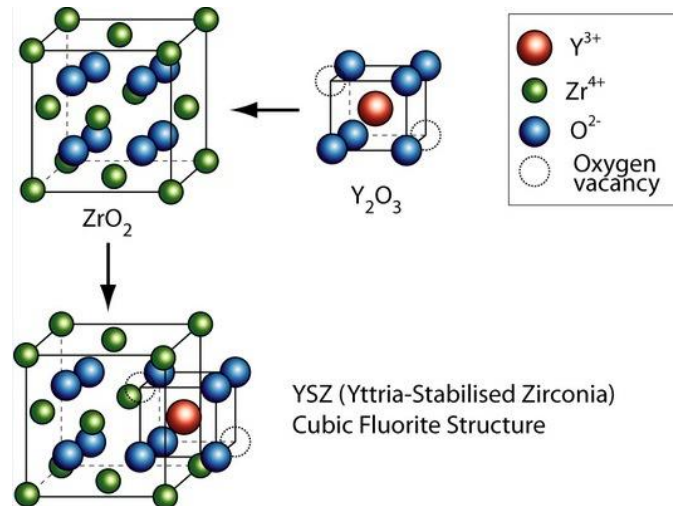
Figure 2.3 Yttria-stabilize zirconia cubic structure

For advantages of YSZ, it's has good ionic conductivity removes need for expensive electro catalysts. YSZ remains solid throughout, electrolyte does not vaporize and minimal corrosion.

For disadvantages of YSZ at high temperature reduces voltage loss due to current which a problem with fuel cells and operation reduces the reaction energy of hydrogen ions and thermal expansion stresses in the material.[29]

YSZ acts as solid electrolyte for oxygen ions and the surface and it's interface with the electrode material play a central role in the relevant reactions: it is involved in the adsorption and oxidation of hydrocarbons, the formation of H_2O and the oxidation of carbon monoxide at the anode as well as the dissociation and incorporation of oxygen at the cathode surface.

2.2 Literature review

Metal oxide films grown by physical vapor deposition (PVD) have been studied for use in solid oxide fuel cells (SOFCs) as thin electrolyte layers. Fuel cells basically use in oxygen-ion conductors, such as stabilized zirconia, have been utilized for electric power generation and developed as future alternatives for vehicle power supplies.[30]

2.2.1 Catalyst Thin films Fabrication Method

There are a number of approaches for thin film fabrication, such as chemical vapor deposition (CVD), spray coating, sol-gel, screen printing, DC magnetron sputtering, thermal evaporation, tape casting, dip-drawing, plaster casting and so on.

Table 2.5 Advantages and disadvantages of catalyst fabrication method

Techniques	Advantages	Disadvantages	Ref.
CVD	- Make a gas-tight - Uniform thin electrolyte film below 5 μm	- Drawbacks of high cost - Low deposition rates - Corrosive gas	[31]
Spray coating	- High deposition rates	- Difficult to obtain a thin dense electrolyte film	[32]
Sol-gel	- Thin dense films	- Time consuming	[33]
Screen-printing	- Reduce cost of fabrication - No risk - Suitable For Small Scale Production	- Low production rate - Difficult to maintain even penetration and print paste	-34] [36
Sputtering	- High deposition rates - High industrial productivity	- Arcing and hysteresis when depositing metal oxide thin films	[37]
Thermal Evaporation	- Low contamination - Improve deposition rate	- Chemical interaction between the charge and cricible	[38]
Tape casting	- Forming uniformly - Inexpensive, scaleable	- Higher crack sensivity	36], [39

For thin film fabrication techniques, R.F. sputtering is a widely used technique and frequently utilized for the production dense, high quality of YSZ thin film electrolytes and crack-free. The advantage of this technique is tailor-made, crack-free film and dense can be obtained[40].

Hong S et al.[41] Present a DC reactive magnetron sputtering by controlling the argon flow rate during process. A $Zr_{84}Y_{16}$ pellet was used. Argon was used as the sputtering gas and O_2 gas was used as the reactive gas. Argon flow rates of 20, 30, 40 sccm was studied. The fuel cells deposited with an argon flow rate of 40 sccm showed unstable behavior because shorting was appeared between electrodes due to the presence of pinholes in the YSZ electrolyte thin film. For argon flow rate of 30 sccm had an OCV value less than the theoretical value for the SOFC and also presence of pinholes at YSZ electrolyte. At deposited with an argon flow rate of 20 sccm had an OCV of 1.09 V, which is nearby the theoretical value and survived to the end of the measurement after 12h as depicted in Figure 2.4.
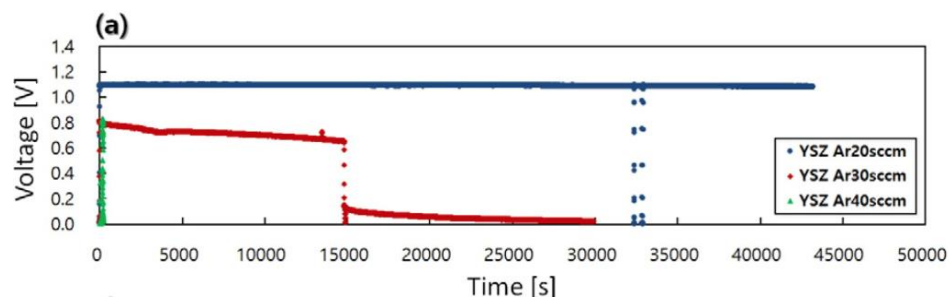
Figure 2.4 Open circuit voltage (OCV) measurements with argon flow rates of 20, 30, and 40 sccm during deposition. OCV measurements maintained for 12 h but only with the lowest flow rate of argon (20 sccm) survived to the end of the measurement[41].

The measured peak power density of the fuel cells with an argon flow rate of 30 sccm was 81 mW/cm^2.   For an argon flow rate of 20 sccm was 158 mW/cm^2 at 450 °C. These differences in the peak power densities were induced by differences in the OCV and the YSZ electrolyte density.
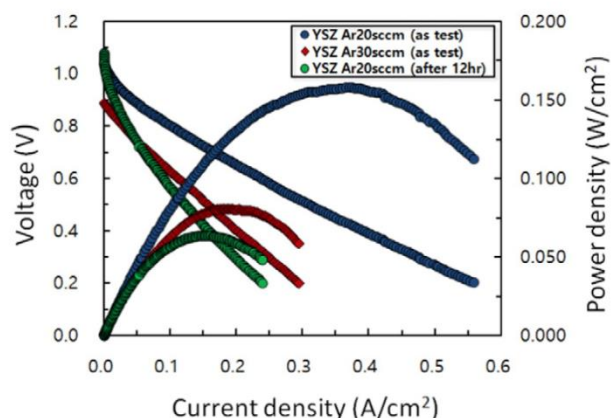
Figure 2.5 Polarization curves of SOFCs with YSZ electrolytes fabricated by argon flow rates of 20 and 30 sccm[41].

The fuel cell fabricated with the lower argon flow rate show highest peak power densities and OCV values. After 12 h the OCV measurement, the performance drop related to the increased cathode resistance is clearly visible.

2.2.2 Composition of Y/Zr

Jankowski A.F. and Hayes J.P.[42] focus on the target synthesis method and the deposition parameters to produce the YSZ films which are synthesized by a homogeneous alloy of Zr-Y is formed to produce an alloy composition of 15at% Yttria. When oxidized, the resulting yttria-stabilized zirconia stoichiometry is $(Y_2O_3)_{0.08}(ZrO_2)_{0.92}$. This 8% yttria composition yields the optimum oxygen-ion conductivity for cubic YSZ at elevated temperatures.[28]

Park Y et al., [43] demonstrate YSZ thin film deposition on alumina substrate in Argon and oxidized at 400-1000 $^{\circ}$C. Y-Zr complex target after deposition of metal film. Five YSZ with varied three compositions of Y/Zr (at %) =4/96, 16/84, 43/57 were prepared. In Figure 2.6, the Nyquist plots (a) Y/Zr=3/97 thickness: 250 nm (b) Y/Zr=3/97 thickness: 50 nm and (c) Y/Zr=16/84 thickness: 320 nm are shown. A large of resistance decrease from 3.67×10^8 Ω (Figure 2.6(a)) to 1.79×10^5 Ω (Figure 2.6(c)) was observed. However, the conductivity (Figure 2.6(c)) with a composition of yttrium concentration increase (Y/Zr=16/84) showed a highest value of conductivity is 3.42×10^{-9} S/cm. Hong et al., [41] and Liu et al.,[44] also used $Y_{16}Zr_{84}$ metallic pellet as the sputtering target. Higher conductivities were observed for thinner films which were thought to be due

to increased oxide conduction along the surface. Increasing the yttrium concentration at the surface also led to higher conductivity.

To observe phase development after oxidation of the Y-Zr thin films, the results XRD patterns are shown in Figure 2.7. At 700 $^{\circ}$C, a clear crystalline phase is find out. The crystalline phase for Y-Zr film is achieved at a lower temperature than alumina thin film because it's inherent high oxygen diffusivity. The observed crystalline peaks matching with combine phase of cubic and monoclinic (Figure 2.7(e)) that explained a crystalline phase of Y_2O_3 and ZrO_2 for a solid solution having a composition in the range of about 3/97 ~ 16/84 of Y/Zr composition[45]. For increasing the yttrium concentration from 3at% (Figure 2.7(e)) to 16at% (Figure 2.7(f)) , the monoclinic phase in oxidized thin film disappears and clear cubic single phase is achieved at 700 $^{\circ}$C for 2 h. as shown in Figure 2.7
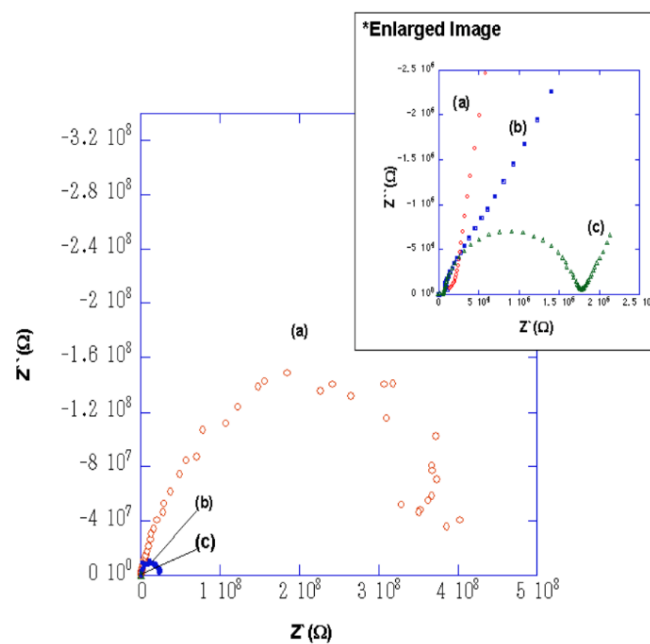
Figure 2.6 The Nyquist plots for Y/Zr

(a) 3/97 thickness: 250 nm   (b) 3/97 thickness: 50 nm   (c) 16/84 thickness: 320 nm
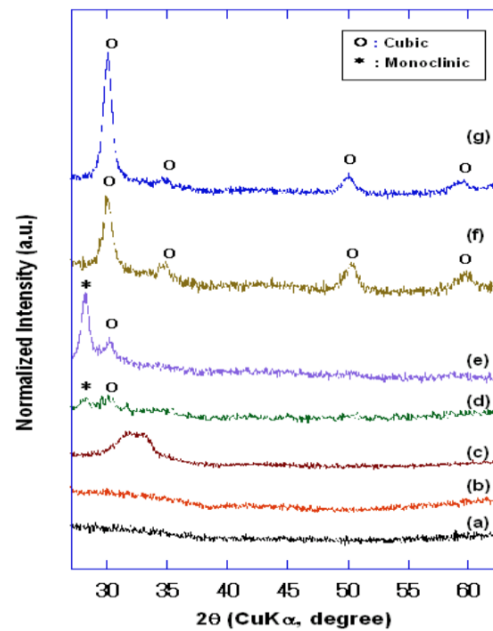
Figure 2.7 XRD patterns for YSZ thin films (a) Substrate at room temperature
(b) Substrate heat-treated at 700 °C for 2 h (c) Y/Zr=3/97 film at room temperature
(d) Y/Zr=3/97 film at 500 °C for 10 h (e) Y/Zr=3/97 film at 700 °C for 2 h
(f) Y/Zr=16/84 film at 700 °C for 2 h (g) Y/Zr=43/57 film at 700 °C for 2 h.

2.2.3 NEMCA

Non-Faradaic electrochemical modification of catalytic activity (NEMCA effect), has been observed for a widely range of gas phase reactions over metals, such as Pt, Pd, Rh, Au, Ag, Ni [46-52] deposited on solid electrolyte. The solid electrolytes commonly used O^{2-} conductors, like YSZ (Y_2O_3-stabilized ZrO_2). A reaction exhibits the NEMCA effect when $|\Lambda| > 1$. When $\Lambda > 1$ the reaction is termed 'electrophobic', while when $\Lambda < -1$ the reaction is termed 'electrophilic' and also 'volcano' and 'inverted volcano' are type of NEMCA behavior as shown in Figure 2.8
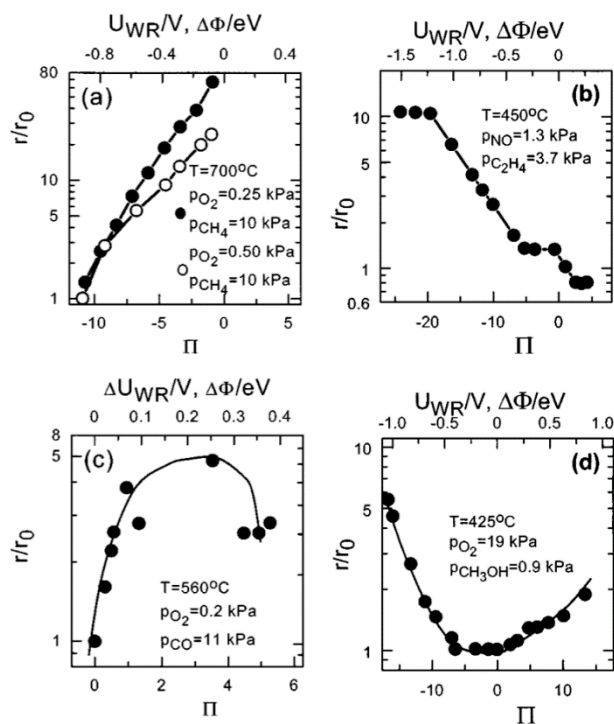
Figure 2.8 Type of electrochemical promotion [23]   (a) Purely electrophobic
(b) Purely electrophilic   (c) Volcano type   (d) Inverted volcano type

Jiménez-Borja C. et al., [53] has been reported the electrochemically promoted combustion of natural gas mainly constituted by methane, ethane and propane at temperature 340 to 420 °C over Pd/YSZ/Au. Methane oxidation exhibited electrophobic behavior, while ethane and propane exhibited inverted volcano behavior[54], as consumption rates were also increasing upon negative polarization. Application of negative overpotentials involved a strengthening of the oxygen chemisorption, leading to an increase of the reaction rate. However, negative overpotentials less exhibited than that observed for positive overpotentials. Because oxygen is more strongly adsorbed on the catalyst surface, a weakening of its chemisorptive bond is expected to have a significant impact on the reaction rate.

The electrochemical promotion of CH_4, C_2H_4, C_2H_6, and C_3H_6 and C_3H_8 oxidation has been investigated on the Pt/YSZ/Au system as shown in Table 2.6

Table 2.6 The electrochemical promotion focus on the Pt/YSZ/Au system

Reaction	Catalyst/electrolyte /electrode	Type of NEMCA	ρ	Λ	Ref.
CH_4	Pt/YSZ/Au	electrophobic	70	13	[55]
C_2H_4	Pt/YSZ/Au	eletrophilic	3	-704	[56]
C_2H_6	Pt/YSZ/Au	eletrophobic	20	500	[57]
C_3H_6	Pt/YSZ/Au	eletrophilic	6	-3000	[58]
C_3H_8	Pt/YSZ/Au	Inverted volcano	1270	40 to 730 -330 to -2330	[54]
C_3H_8	Pt/YSZ/Au	electrophobic	5.6	330	[24]
C_3H_8	Pt/YSZ/Au	electrophobic	7.8	480	[25]
C_3H_8	Pt/YSZ/Au	electrophobic	2	1650	[59]

Marwood and Vayenas achieve the "wireless" technology in which a platinum film is deposited on a YSZ pellet side between two gold electrodes [60] shown in Figure 2.9. A bipolar configuration allows the polarization of the catalytic layer without any direct electrical connection[61]. To make a YSZ thin film by wireless technology. YSZ deposited on substrate, while two Au films deposited on left and right side of obtained YSZ thin film.
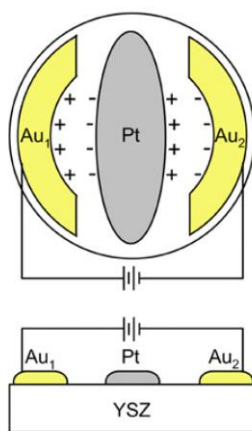
Figure 2.9 The bipolar cell [61]

Shunsuke Akasaka [62] was studied a YSZ thin film based limiting current-type oxygen and humidity sensor on silicon substrate. Pt pad electrode and Pt wiring connected to the Pt pad electrode. An 8% YSZ electrolyte was deposited by RF sputtering. Ar gas is in the sputtering chamber. The YSZ film growth rate increases as the Ar gas pressure decreases. Considering that a current plateau is observed in dry air. The current plateaus at the lower and higher voltage regions correspond to the reduction of oxygen and water vapor, respectively. (Figure 2.10 and Figure 2.11)
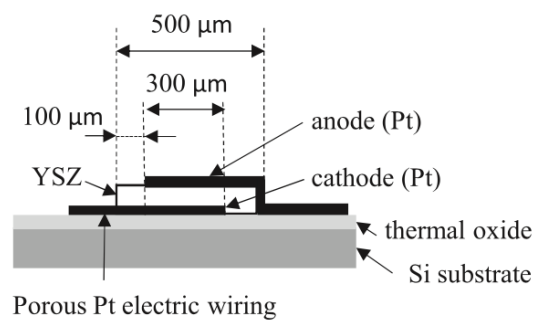
Figure 2.10 Structure fabricated on a silicon substrate.
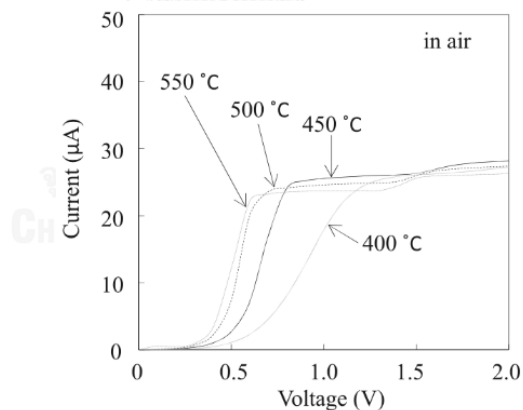
Figure 2.11 Voltage-current Characteristics between 400-550 °C

Hong S et al.,[63] fabricated dense thin film YSZ electrolytes on alumina substrate by sputtering at 4:1 and 13:1 different ratio of Ar/O_2 gas sputtering mixture. For electrochemical characterization show the ionic conductivity data of YSZ thin film. Moreover to enhanced ionic conductivity, it is more important to have pinhole-free thin film electrolyte in order to avoid electrical shorting which dramatically kills the fuel cell performance during the operation. The polarization behaviors and EIS results

of the fuel cell samples with YSZ electrolytes fabricated under 4:1 and 13:1 ratio of Ar:O_2 are shown in Figure 2.12. The open circuit voltage (OCV) of sample was measured as 1.01 V which is near the theoretical value of the SOFC. Ar:O_2 13:1 showed electrical shorting behavior while the other sample showed stable performance.
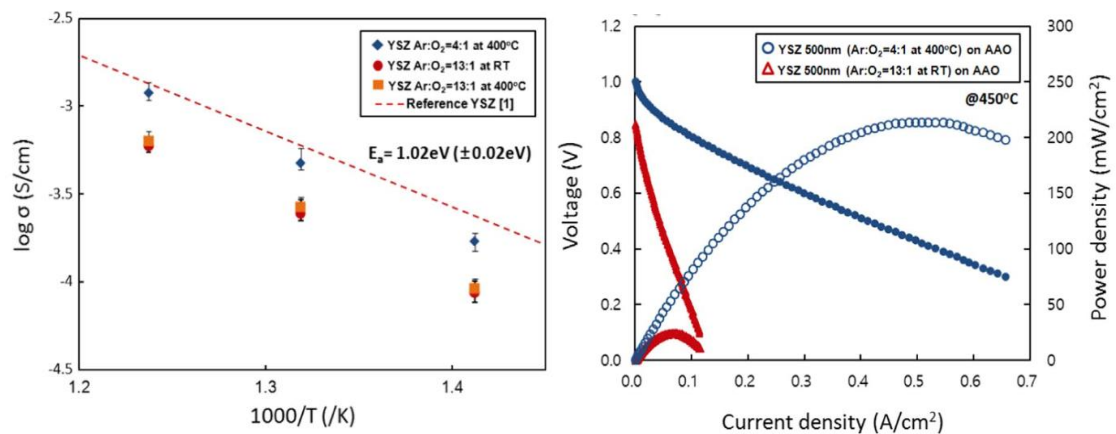
Figure 2.12 (a) Polarization curves of fuel cells with YSZ electrolytes fabricated under 4:1 and 13:1 ratio of Ar:O_2 conditions measured at 450 ˚C. (b) EIS spectra of the fuel cell with YSZ electrolytes fabricated under 4:1 ratio of Ar:O_2 measured in different voltage condition.

CHAPTER III

METHODOLOGY

3.1 Catalyst preparation

3.1.1 Sputtering of YSZ films

YSZ thin films were deposited using RF magnetron sputtering (Oerlikon Univex 350 sputtering system). The target was zirconium yttrium (Zr_{84}/Y_{16} at%) alloy sputtering target of 50.8 mm diameter and 6.35 mm thickness (99.9% purity, Edgetech industries) and the substrate were alumina disks of 20 mm diameter and 1.2 mm thickness (sliced from alumina rods, Coorstek Inc).

The RF sputtering power has maximum power 600 W, and the source-to-substrate distance was 10 cm. The vacuum reached 1.2×10^{-4} mbar and the argon flow rate was set to 20 sccm. The sputtering time was varied. ZrY alloy deposited on alumina substrates appeared metallic silver but became glassy transparent after calcination in air to form YSZ at 700 °C for 2 h [43]. The temperature was set so to reduce the monoclinic phase and promote only the cubic phase.

The Oerlikon 350 single-chamber sputtering system is equipped with two RF sputtering guns. The sputtering process yields are greatly improved by the use of the magnetron, which uses magnetic fields to confine the plasma's electrons and increases the energy of the incident ions (Ar^+) to the sputter target. The substrate can be rotated up to 20 RPM for improved uniformity.

SEM micrographs of the deposited YSZ films were taken by JEOL mode JSE-6400 scanning electron microscope and Link Isis Series 300 programmed energy dispersive x-ray spectroscopy (EDX) for the determination of elemental distribution.

3.1.2 Wireless experiment

Pt was deposited on the obtained YSZ thin films by wet impregnation. Two gold electrodes were sputtered on two opposite segments on the obtained YSZ thin films by sputtering (JOEL:JFC-1100E Ion sputtering).

Pt deposited on YSZ thin film via wet impregnation

Au electrode by sputtering
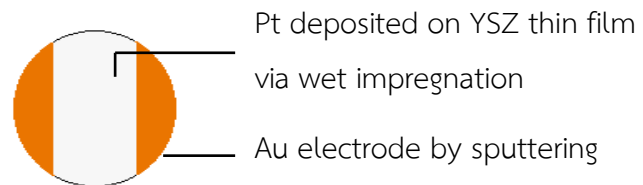
Figure 3.1 Wireless experiment (top view)
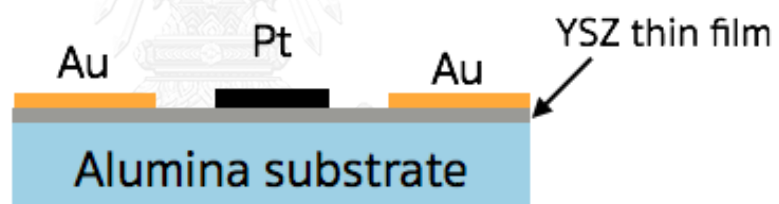
Figure 3.2 Wireless experiment (cross-sectional view)

3.1.3 Conventional experiment

Gold paste was deposited on alumina substrate by screen-printing. This ink is dried at 100 – 150 °C for 10 - 15 min in a box oven and typically fired at 800 °C for 1 hour in an oxidizing atmosphere to ensure adhesion prior to testing at the desired test temperature. Gold is deposited on the substrate first prior to the metal deposition. ZrY was deposited on half of gold and calcined in air 700 °C for 2 hr. Pt was deposited after layer of cell form in YSZ thin film. Pt was deposited by sputtering.
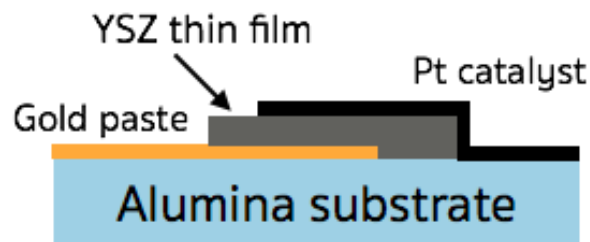
Figure 3.3 Conventional experiment

3.2 Cell testing

3.2.1 NEMCA experiment

NEMCA of propane oxidation was studied under a stoichiometric ratio of propane to oxygen, 1 kPa of C_3H_8 and 5 kPa of O_2 balanced with He, at 200-500 °C, at atmospheric pressure and with electric potential in the range of 0-30 V by a power supply connected to a multimeter for current readings. The reaction gases were mixtures of propane , oxygen and helium as the vector gas. The gas composition was controlled by mass flow controllers. The reaction products were analyzed by an online IR spectrometer for CO_2 concentrations data. which could be calculated into faradaic efficiency and rate enhancement ratios by using equation (4) and (5), respectively. The diagram of the experimental is shown in Figure 3.3

$$\Lambda = (r- r_0)/(I/nF) \tag{4}$$

$$\rho = r/r_0 \tag{5}$$

where r is the electropromoted catalytic rate

r_0 is the open-circuit rate, i.e. non-promoted catalytic rate

I is the applied current

n is the charge of the promotion ion

F is Faraday's constant (96485 C/mol)
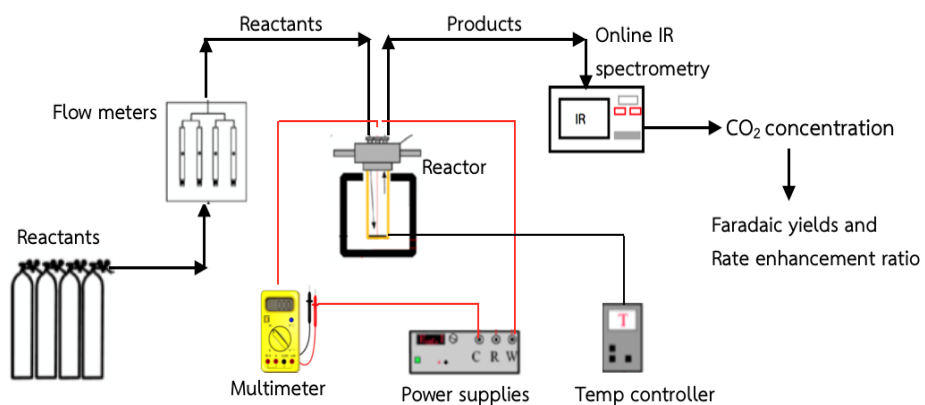
Figure 3.4 Schematic diagram

3.3 Procedures of propane oxidation

```
                    ┌─────────────────────────┐
                    │          NEMCA          │
                    └─────────────────────────┘
                                 │
                                 ▼
          ┌───────────────────────────────────────────┐
          │           Catalyst preparation            │
          │  "YSZ thin film on alumina substrate"     │
          └───────────────────────────────────────────┘
                                 │
                                 ▼
                    ┌─────────────────────────┐
          ┌─────────│    Propane oxidation    │─────────┐
          │         └─────────────────────────┘         │
          ▼                                             ▼
  ┌─────────────────┐                       ┌─────────────────────────────┐
  │      Vary       │                       │            Vary             │
  │ Potential 0 – 30 V │                    │   Temperature 200 – 500 °C  │
  └─────────────────┘                       └─────────────────────────────┘
          │                                             │
          └──────────►┌───────────────────────────┐◄───┘
                      │     Faradaic efficiency    │
                      │ and rate enhancement ratio │
                      └───────────────────────────┘
                                 │
                                 ▼
                      ┌───────────────────────────┐
                      │      Characterization      │
                      │         SEM & EDX          │
                      └───────────────────────────┘
```
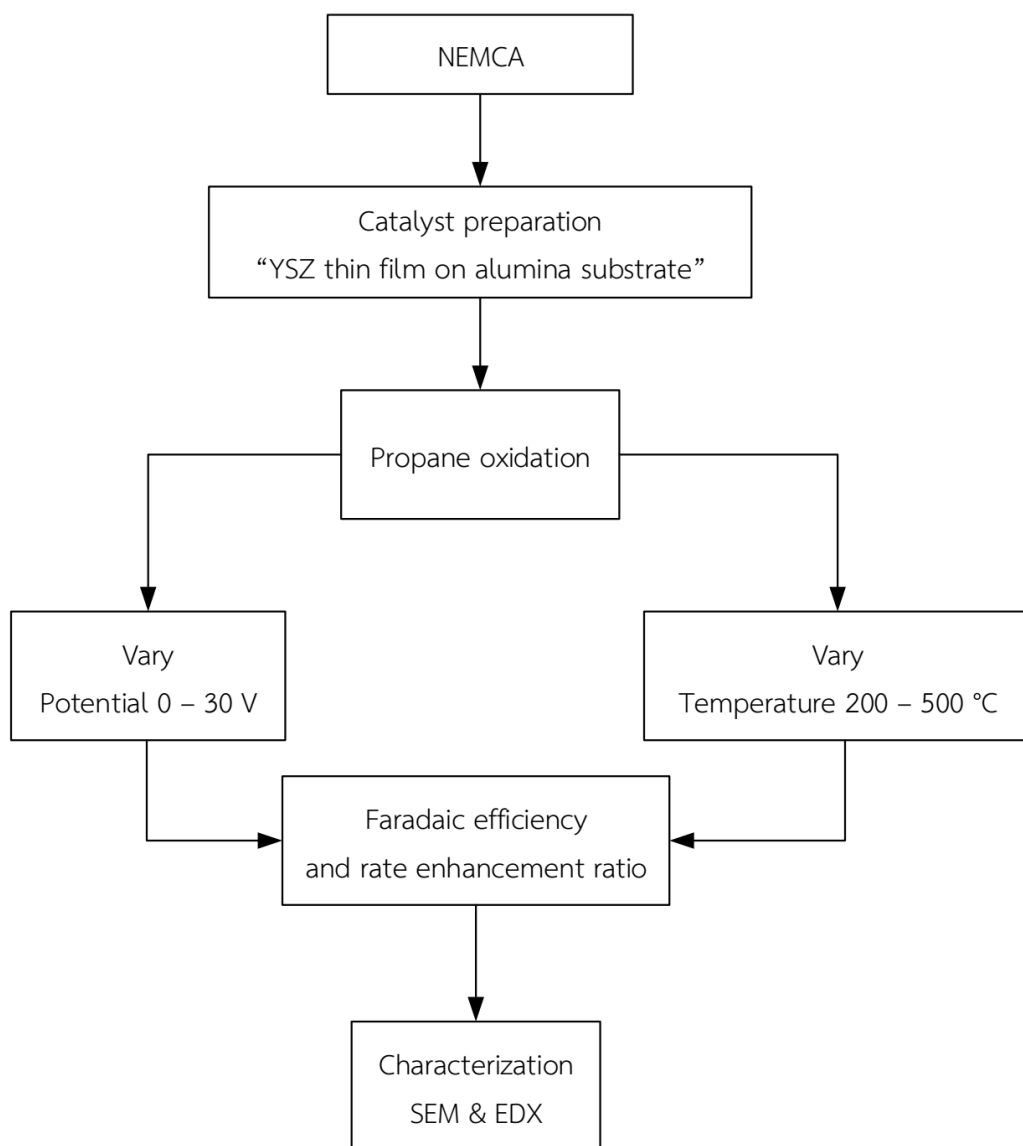
Figure 3.5 Procedures of propane oxidation

CHAPTER IV
RESULTS AND DISCUSSION

Electrochemical promotion of propane combustion was experimented. YSZ thin-film cell on alumina was studied in different preparation methods, the effects of potential differences and temperature on reaction rate were studied as well.

4.1 Effects of Sputtering Conditions

Sputtering is a physical vapor deposition technique in which the material to be deposited is transported from a source to the wafers. Function of RF magnetron sputtering UNIVEX 350 includes power, gas flow rate and operating time. To study the effects of sputtering condition, EDX characterization was used as shown in Table 4.1.

Table 4.1 indicates elements of ZrY on alumina disk in different RF power, i.e. 100 W and 150 W, at constant Ar flow rate of 40 sccm for 45 minutes. An increase in target power causes an increase in content of Zr and Y.

Table 4.1 EDX characterization of ZrY on alumina disk in RF 100 W and 150 W at constant Ar flow rate of 40 sccm

Element (at%)	Ar 40 sccm	
	RF 100 W	RF 150 W
OK	65.5	59.78
AlK	34.07	37.15
YL	00.09	01.12
ZrL	00.34	01.95

According to Table 4.2, the ZrY on alumina varied in different Ar flow rate, i.e. 20 sccm, 40 sccm and 60 sccm, at constant RF power of 250 W. The increase of Ar gas flow rate resulted in the decrease in content of Zr and Y on alumina. Therefore, flow rate at 20 sccm is the suitable flow rate to perform sputtering.

Table 4.2 EDX characterization of ZrY on alumina disk in different Ar flow rate; 20, 40, 60 sccm at constant RF power of 250 W

Element (at%)	RF 250 W		
	Ar 20 sccm	Ar 40 sccm	Ar 60 sccm
OK	57.95	60.11	62.47
AlK	38.05	39.18	37.14
YL	01.45	00.19	00.12
ZrL	02.55	00.53	00.27

In conclusion, decrease in flow rate of Ar will increase the deposition of ZrY, by observing from the change in optical property of alumina which transformed from transparent to opaque.

To compare effects of the applied potentials and temperatures on catalytic CO_2 production rate, RF power and time of sputtering were varied at 0 to 30 volts and 200 to 550 °C, respectively.

4.2 Catalytic activity under open-circuit condition via wireless method

The electrochemical performances for the propane reaction were investigated under various atmospheric conditions including O_2 balance He, pure He, and C_3H_8 balance He. The catalytic reaction rate was experimented at 200-550 °C at different RF power and sputtering time. Sputtering power and time were varied at 400 W for 4 h, 200 W for 4 h and 200 W for 8 h. The catalytic reaction rate under open circuit (i.e. with no current passing through the electrolyte) was increased from 6.61×10^{-10} to 1.56×10^{-8} mol/s for 400 W for 4 h, from 4.62×10^{-9} to 6.39×10^{-9} mol/s for 200 W for 4 h and from 2.2×10^{-10} to 1.17×10^{-8} mol/s for 200 W for 8 h, while the temperature was increased from 200 to 550 °C as shown in Figure 4.1 to 4.3. The results reveal that at 400 W for 4 h sputtering condition, the catalyst exhibited high CO_2 production rates due to bombardment of the target by high energetic particles onto a substrate.
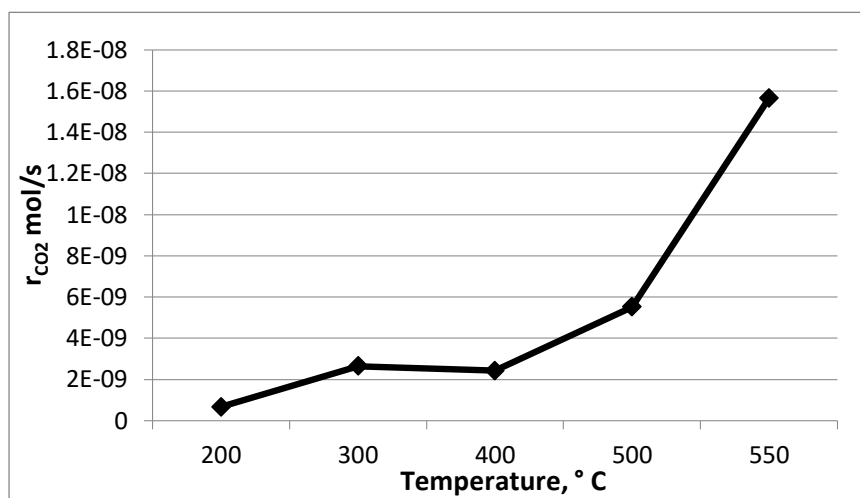
Figure 4.1 CO_2 production rates under open-circuit at sputtering power of
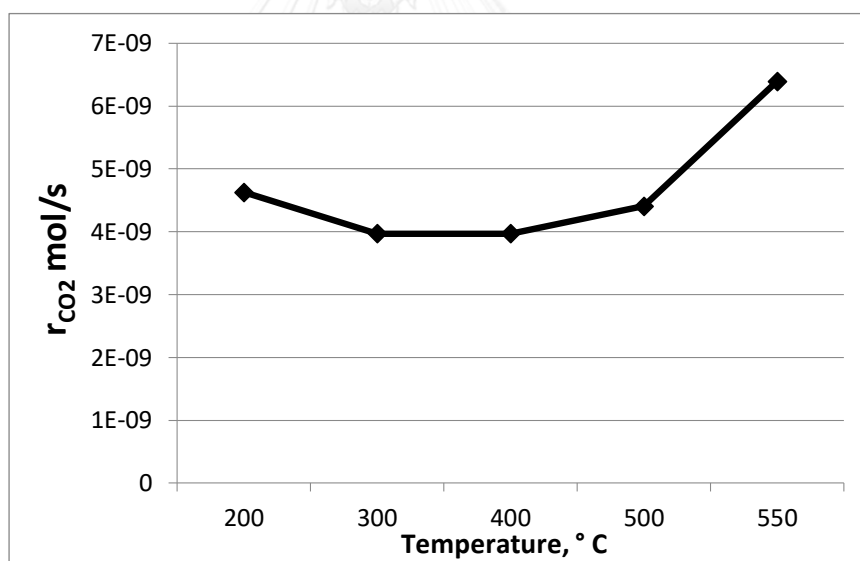
400 W for 4 h

Figure 4.2 CO_2 production rates under open-circuit at sputtering power of
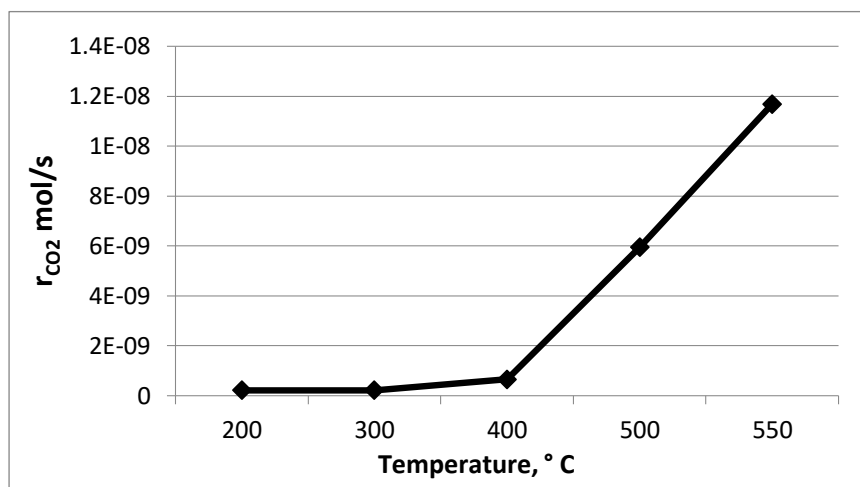
200 W for 4 h

Figure 4.3 CO_2 production rates under open-circuit at sputtering power of 200 W for 8 h

4.3 Catalytic activity under closed-circuit condition via wireless method

The application of potential to the catalyst affects the activity of Pt deposited on alumina substrate. The catalytic activity of Pt for the propane oxidation can be promoted when a voltage is applied between the two gold electrodes.

Figure 4.4 shows effects of the applied potential and temperature on catalytic CO_2 production rate at sputtering power of 400 W for 4 h. The results shows the closed-circuit catalytic CO_2 production rates which increase from 6.61×10^{-10} to 1.98×10^{-8} mol/s, while the temperature increases from 200 to 550 °C. The corresponding maximum rate enhancement ratios are 4.33, 1, 1, 1.04 and 1.26 at 200, 300, 400, 500 and 550 °C, respectively.

Figure 4.5 and Figure 4.6 show the closed-circuit catalytic CO_2 production rates, at sputtering power of 200 W for 4 h and 200 W for 8 h which increase from 4.62×10^{-9} to 6.83×10^{-9} mol/s and 2.2×10^{-10} to 1.23×10^{-8} mol/s, respectively. The corresponding highest rate enhancement ratios are 1, 1, 1, 1.2, 1.06 and 3, 1, 1, 1.07, 1.05 at 200, 300, 400, 500 and 550 °C, respectively.

In case of different RF power at constant time, the highest catalytic CO_2 production rate is 1.98×10^{-8} mol/s operated by sputtering at 400 W, while in case of

different time at constant power, the highest catalytic CO_2 production rate is 1.23×10^{-8} mol/s operated by sputtering for 8 h. The CO_2 production rate is not affected by changing the applied potentials. Consequently, the lower operating power of sputtering is experimented because it decreases arcing in sputtering process.

The catalytic activity by wireless method cannot be found the current data probably due to wireless ones correspond to situations where platinum is not used as an electrode and is electronically isolated with voltage passing between the gold electrod. Part of the platinum film is therefore polarized with positive charge while the other part is polarized with negative charge. Thus, there is not a uniform catalyst work function as in the case when platinum is used as the working electrode. According to the theory, the wireless method could produce an infinitesimal value of current, but the present experiment is insufficient to detect the current.

Current bypass may be the main problem to be encountered in the design and operation of such "wireless" NEMCA catalysts, consisting of two electrically biased electrodes with a large number of thin catalyst stripes or individual microscopic catalyst particles supported on electrolyte between the two end electrodes. [64]

Figure 4.4 CO_2 production rates under closed-circuit at sputtering power of 400 W for 4 h under various operating temperature of 200-550 $^\circ$C
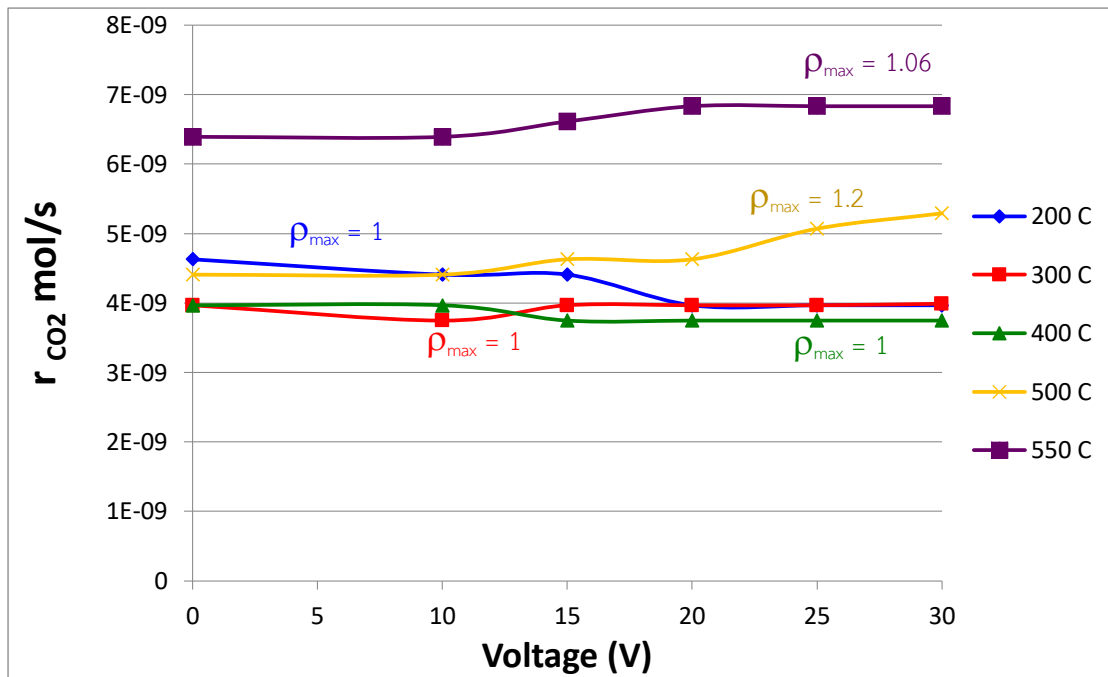
Figure 4.5 CO_2 production rates under closed-circuit at sputtering power of 200 W for 4 h under various operating temperature of 200-550 °C

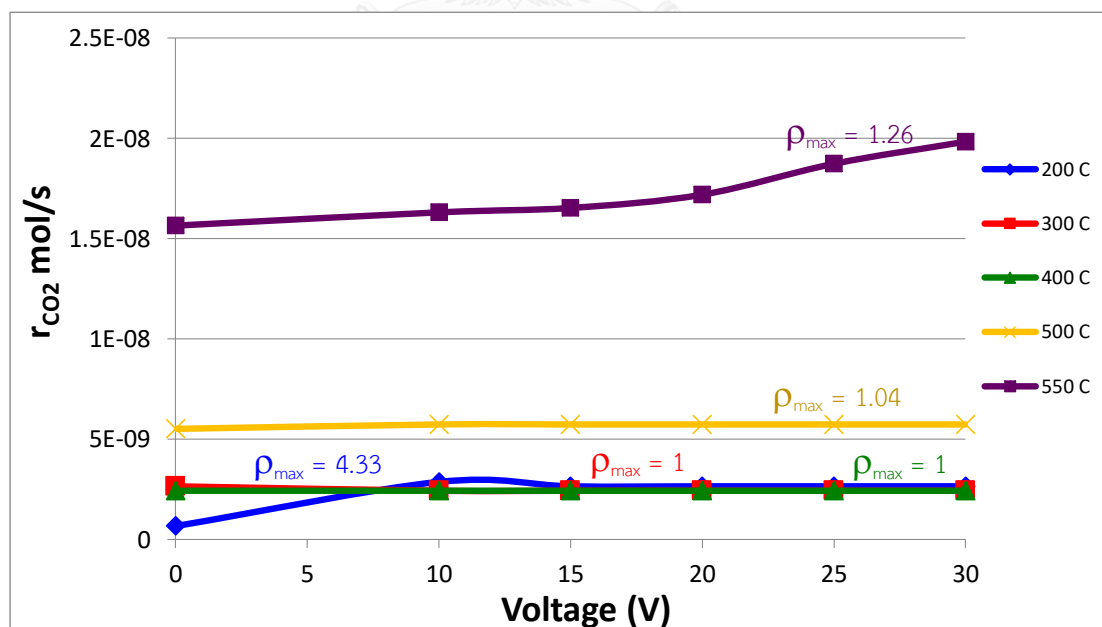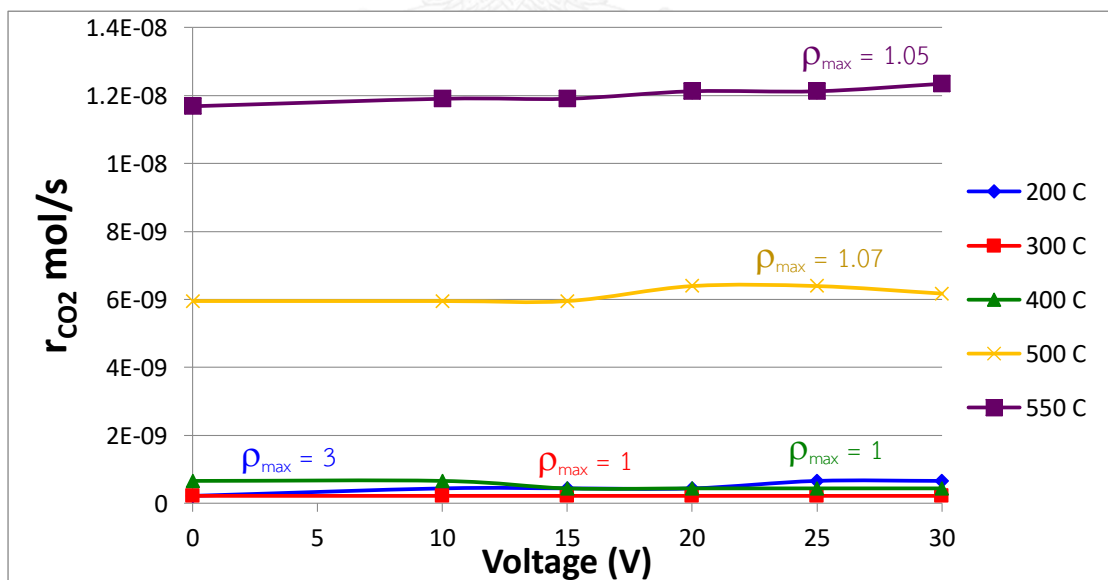**Figure 4.6** CO_2 production rates under closed-circuit at sputtering power of 200 W for 8 h under various operating temperature of 200-550 °C

4.4 Catalytic activity under closed-circuit condition via conventional method

The catalytic activities of the Pt/YSZ system in the oxidation of C_3H_8 under various operating temperature of 200-550 °C are shown in Figure 4.7 to 4.10. The catalytic activity measurements were performed by conventional method with both co-fed reactants as gaseous C_3H_8 and O_2. Under closed circuit, the cell reactor operated as an electrochemical oxygen pump. A current was imposed through the oxygen ion (O^{2-}) conducting electrolyte.

4.4.1 Fabrication by 'Au paste - YSZ thin film – Pt'

Figure 4.7 shows the faradaic efficiency and rate enhancement ratios at 200 °C. Under an open circuit (I=0), a stable steady-state rate of 3.53×10^{-9} mol/s was obtained. By imposing a voltage of 0.1-0.2 V, the faradaic efficiency and rate enhancement ratios were increased to 0.21 and 1.13, respectively. However, when the voltage was increased to 0.7 V, the faradaic yield and rate enhancement ratios were decreased. However, the voltage cannot be increased over 0.7 V due to appearance overload of current from multimeter measurement.

As the temperature was increased to 300 °C and 400 °C, the faradaic efficiency and rate enhancement ratios were increased to 0.41 and 1.11, respectively for temperature at 300 °C, and increased to 0.5 and 1.05, respectively for temperature at 400 °C while applying a voltage of 0.1 V. When voltage was increased, the faradaic efficiency and rate enhancement ratios were decreased because the cell reaction respond only at low voltage after the cell had stable rate under open-circuit at 4.18×10^{-9} mol/s and 9.48×10^{-9} mol/s at temperature 300 °C and 400 °C as shown in Figure 4.8 and 4.9, respectively.

Figure 4.10 shows the faradaic efficiency and rate enhancement ratios at temperature 500 °C. The highest value of faradaic efficiency is 1.87 at applied voltage of 0.1 V. The faradaic efficiency tends to decrease when higher voltage was applied due to increasing current that follow up with voltage. However, the rate enhancement ratios increased as the cell voltage was increased with the maximum value reaching to 1.22 when increased voltage to 0.9 V.

For fabricating the thin film cell by Au paste-YSZ thin film-Pt, the observed electrochemical promotion behavior is unavailable due to faradaic efficiency parameter not exceed 1 because a catalytic reaction exhibits the NEMCA effect when $|\Lambda| > 1$. It has only one value at 0.1 V at temperature 500 °C, which exhibits the NEMCA effect while other temperature shows a value of Λ lower than 1 because of fracture in calcination process of YSZ thin film from ZrY sputtering on Au electrode, as a result, cell reaction cannot exhibit NEMCA behavior and faradaic efficiency that not exceed 1.

Figure 4.7 Faradaic efficiency and rate enhancement ratio vs applied voltages at 200 °C using Au paste-YSZ thin film-Pt

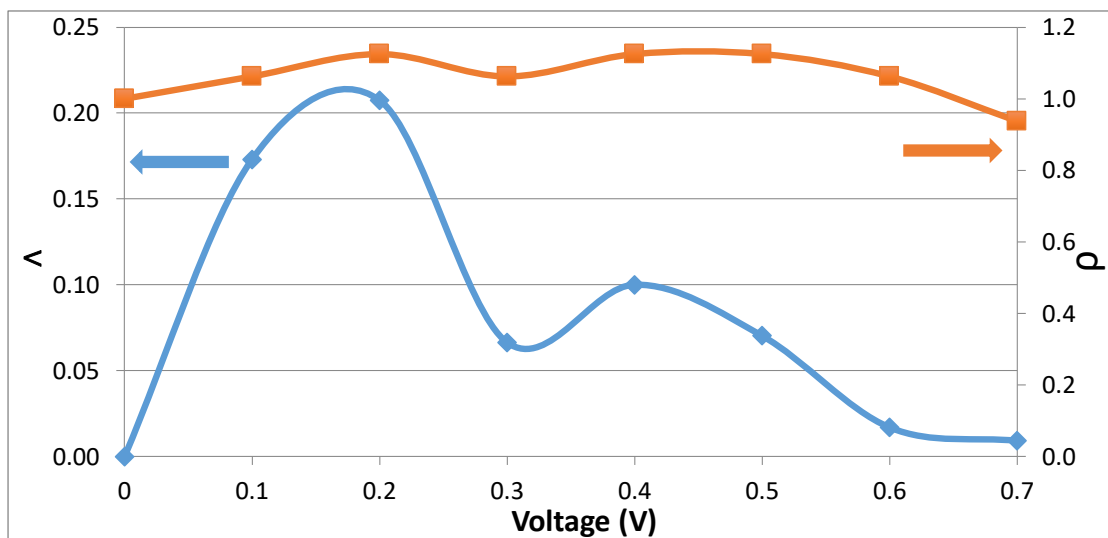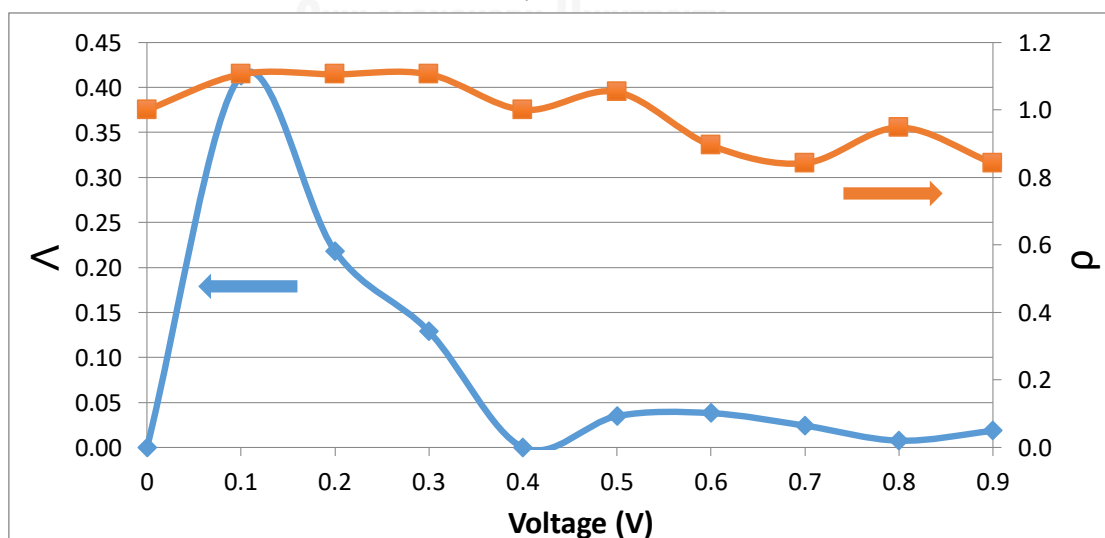**Figure 4.8** Faradaic efficiency and rate enhancement ratio vs applied voltages at 300 °C using Au paste - YSZ thin film – Pt
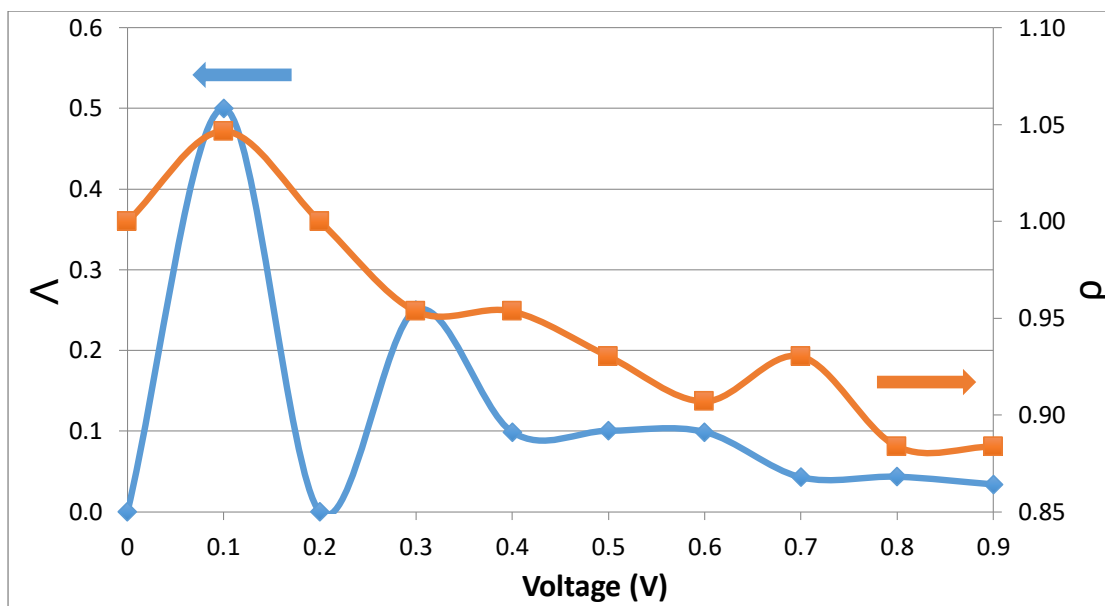
Figure 4.9 Faradaic efficiency and rate enhancement ratio vs applied voltages at
400 °C using Au paste - YSZ thin film – Pt

Figure 4.10 Faradaic efficiency and rate enhancement ratio vs applied voltages at
500 °C using Au paste - YSZ thin film – Pt

4.4.2 Fabrication by 'Au paste – YSZ (O$_2$) thin film – Pt'

  In the earlier fabrication by conventional method, which used ZrY sputtering target and calcined at 700°C in air to form YSZ thin films, the cell cannot exhibit NEMCA behavior. To improve cells performance, a homogeneous alloy of ZrY is processed into a planar magnetron target. The ZrY alloy target composition is designed to maximize the ion conductivity of the deposited YSZ as an electrolyte layer. The deposition chamber is cryogenically pumped from atmospheric pressure to a base pressure of 5 x10^{-5} mbar within 40 minutes which includes a 1.2x10^{-2} mbar vacuum. ZrY target is sputtered with an argon-20% oxygen gas mixture to form thick Zr-Y-O films. The substrates are positioned horizontally 10 cm away from the center of the sputter deposition target at power of 200 W.

  Figure 4.11-4.14 contain data obtained with the cell operating under closed circuit using YSZ thin film synthesized by an argon-20% oxygen gas feed mixture in sputtering process without calcination procedure. The figures show the effect of voltage, the electrical potential difference between the working (Pt) and counter electrode (Au paste), on the dimensionless parameter faradaic efficiency, Λ and rate enhancement ratios, ρ with temperature at 200 to 500 °C. In figure 4.11-4.13, the reaction rates are decreased at forward scanning (O^{2-} pumped towards the catalyst) while in the reverse scanning, the reaction rate still decreased continuously. This exhibited the 'electrophilic' type of NEMCA, which can be attributed not only to the electrochemically induced decrease in oxygen coverage and enhancement of propane chemisorption[65], but also to partial reduction of the surface upon electrochemical pumping of oxygen away from the catalyst[66]. The faradaic efficiency has the negative value due to %CO$_2$ concentration less than open-circuit voltage. At the operating temperature of 500 °C, rate enhancement ratios, ρ increased at both forward and reverse scanning as shown in Figure 4.14. The reaction exhibits the usual electrophobic behavior observed in a large number of NEMCA studies[67]. The faradaic efficiency was obtained, showing a number of values which exceed 1. At the operating temperature of 200 °C - 400 °C the effect is hardly faradaic.

The rate enhancement ratios decreased between 200 °C – 400 °C and the faradaic efficiency is hardly consistent probably due to Au paste counter electrode in term of unevenness of surface in screen-printing process which resulted in non-consistent of current and concentration of CO_2 is reduced. Another problem encountered after calcination process, was Au paste falling off alumina substrate, therefore, it is difficult to control the uniformity of the surface.

Figure 4.11 Faradaic efficiency and rate enhancement ratio vs applied voltages at 200 °C using Au paste – YSZ(O_2) thin film – Pt

Figure 4.12 Faradaic efficiency and rate enhancement ratio vs applied voltages at 300 °C using Au paste – YSZ(O_2) thin film – Pt

Figure 4.13 Faradaic efficiency and rate enhancement ratio vs applied voltages at 400 °C using Au paste – YSZ(O_2) thin film – Pt
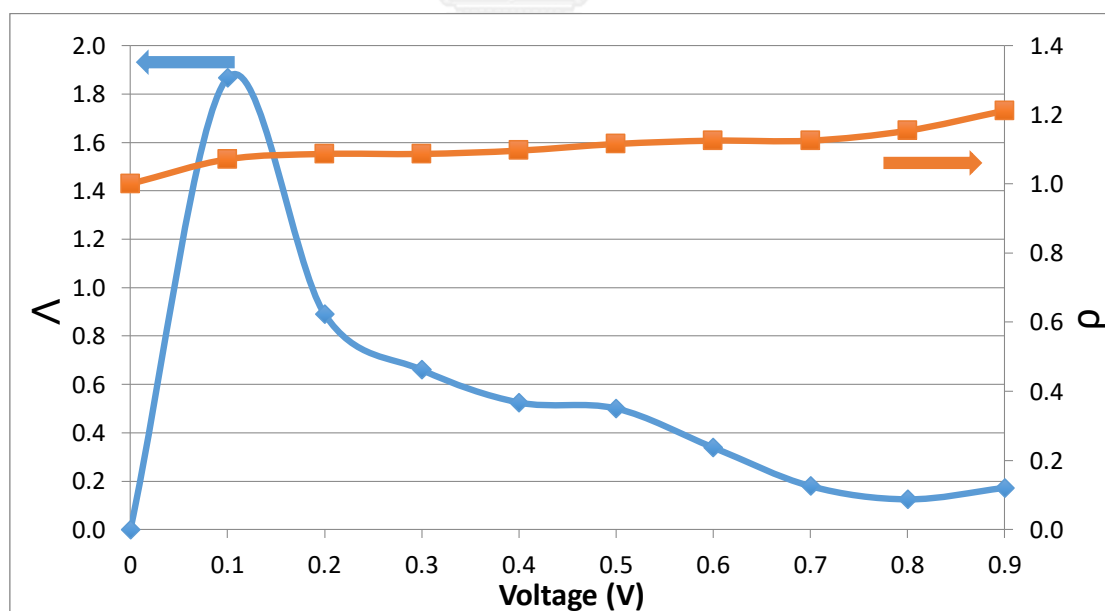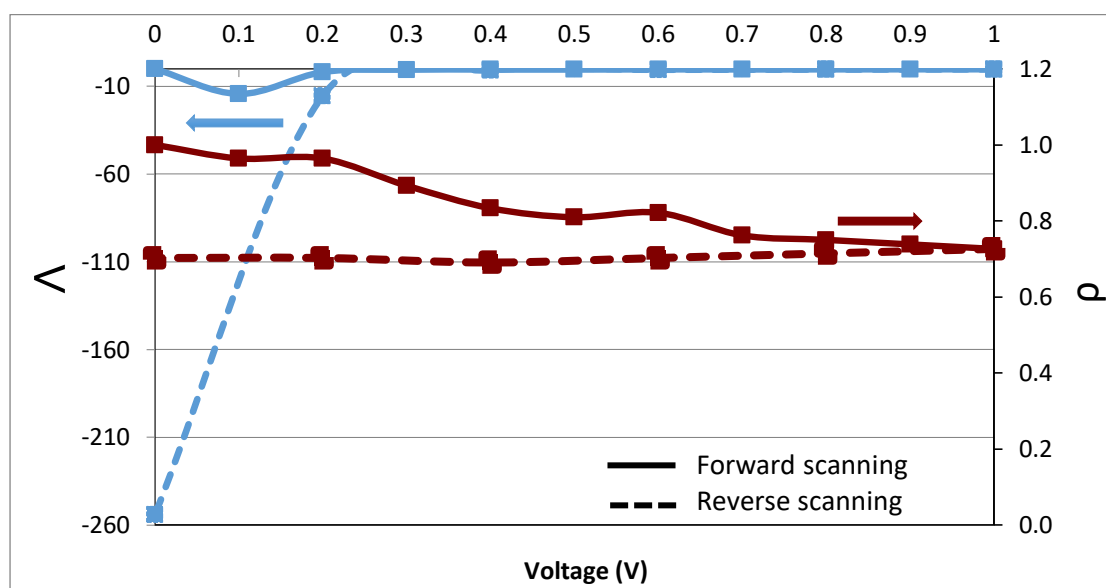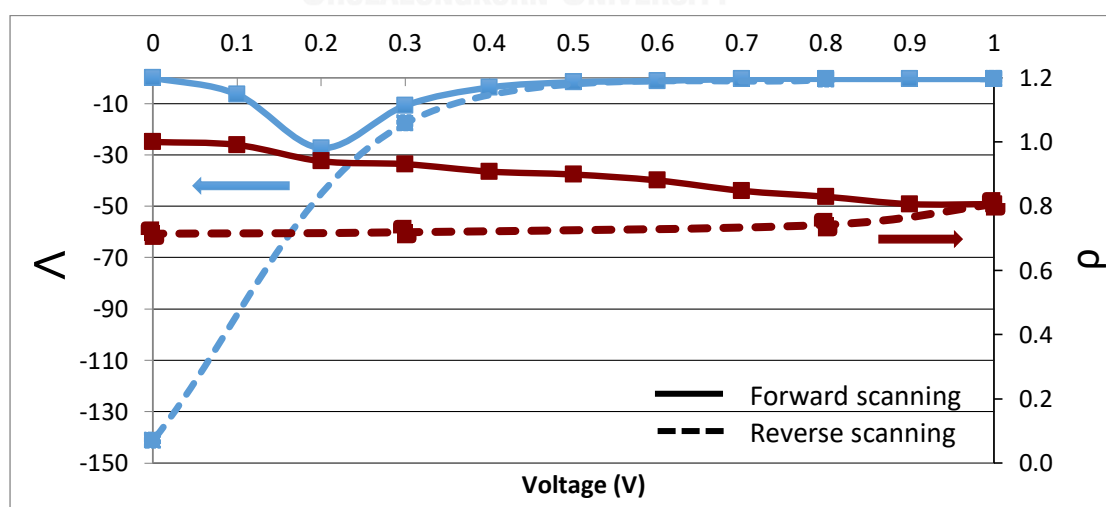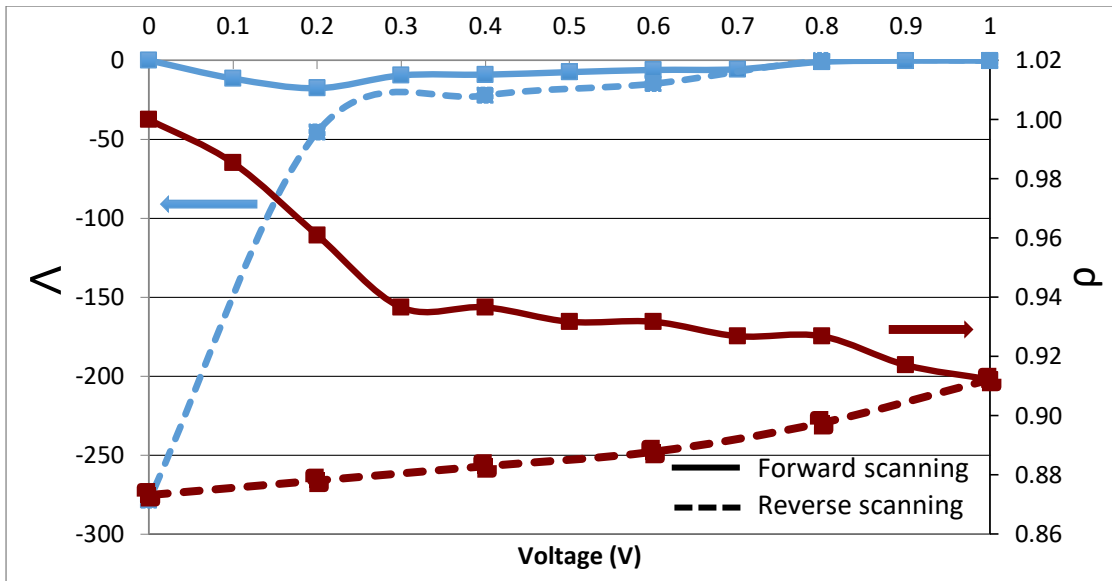

Figure 4.14 Faradaic efficiency and rate enhancement ratio vs applied voltages at 500 °C using Au paste – YSZ(O_2) thin film – Pt

4.4.3 Fabrication by 'Au sputter – YSZ (O$_2$) thin film 4 h– Pt'

The Au paste change into Au sputtered counter electrode resulted in smooth surface which attached to the substrates tightly. The YSZ thin film fabrication is similar to previous experiments, Ar/O$_2$ mixture as sputtering gas with the same plasma power conditions mentioned above in operating time for 4 h.

From Figure 4.15, the results from the forward and reverse scanning presented a much higher NEMCA behavior than previous experiments, the higher faradaic efficiency; Λ values are observed at 0.1 – 0.7 V and 0.1-0.5 V in forward and reverse scanning, respectively. The increase in reaction rate is more profound at forward scanning while stable reaction rates are obtained at reverse scanning.

At 300 °C (Figure 4.16), shows the faradaic efficiency parameter values exceed 1 at low potentials (lower than 0.4 V). However, the reverse scanning did not exhibit the NEMCA effect. This performance is also observed at either forward or reverse scanning at 400 °C as shown in Figure 4.17. However, the reaction rate can be reversed for both temperature at 300 °C and 400 °C. At 300 °C, the highest reaction rate is constant in the range of 0.2 – 0.7 V for only forward scanning while at 400 °C, the reaction rate is constant in the range of 0.1 – 0.7 V in both forward and reverse scanning.

At 500 °C (Figure 4.18), shows the same effects of potential on Λ and ρ at Au paste – YSZ(O$_2$) – Pt. The behavior compared with previous experiment at 500 °C is the same qualitatively, but not quantitatively. Much lower Λ values were obtained because active sites of catalyst on Pt surface are lower than those of the previous experiment. Nevertheless the reaction rate has the same trend either at forward or reverse scanning. An explanation of this phenomenon is the temperature effect cause at high temperature, %CO$_2$ concentration tend to increase continuously. Therefore, in order to study the temperature effect on cell reaction, the cell was cool down to room temperature then raise the cell temperature to 500 °C again. The active catalyst was activated. The faradaic and rate enhancement ratio parameter still showing the same behavior. It can reproduce. The error bar was presented on graph. This ensures that temperature affected the cell reaction. To affirm the reaction rate performance,

IR spectroscopy intensively record the dependence of CO_2 concentration (%vol) on time (second) to show step change between steady open-circuit and close-circuit varied with forward scanning as shown in Figure 4.19. However, some data points may not be consistent with the majority because the recorder show delicate data in every second and due to some errors from the system and background noise from the environment.

Figure 4.15 Faradaic efficiency and rate enhancement ratio vs applied voltages at 200 °C using Au sputter – YSZ(O_2) thin film sputtered for 4 h – Pt

Figure 4.16 Faradaic efficiency and rate enhancement ratio vs applied voltages at 300 °C using Au sputter – YSZ(O_2) thin film sputtered for 4 h – Pt

Figure 4.17 Faradaic efficiency and rate enhancement ratio vs applied voltages at 400 °C using Au sputter – YSZ(O_2) thin film sputtered for 4 h– Pt
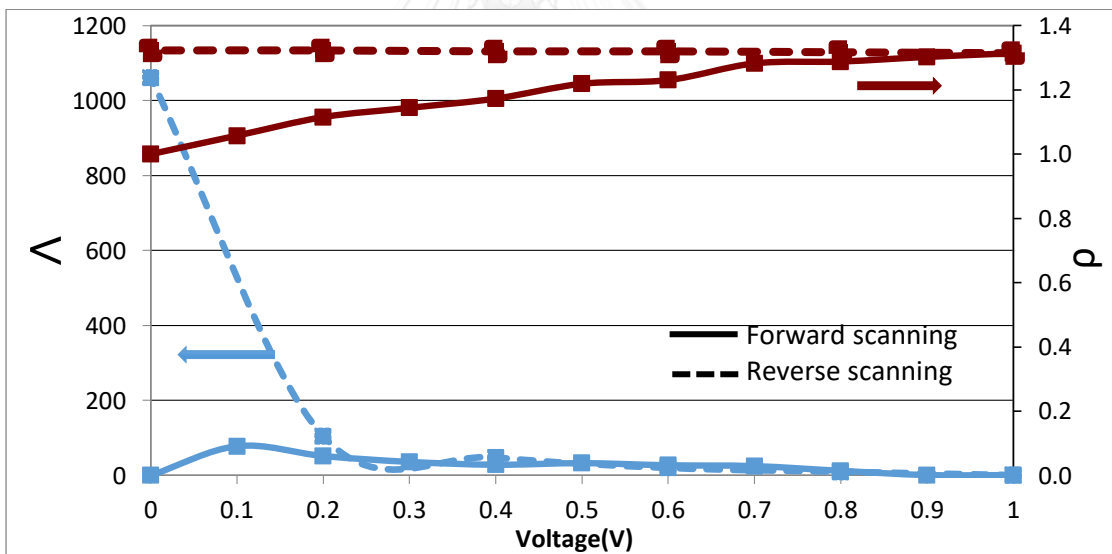

Figure 4.18 Faradaic efficiency and rate enhancement ratio vs applied voltages at 500 °C using Au sputter – YSZ(O_2) thin film sputtered for 4 h – Pt
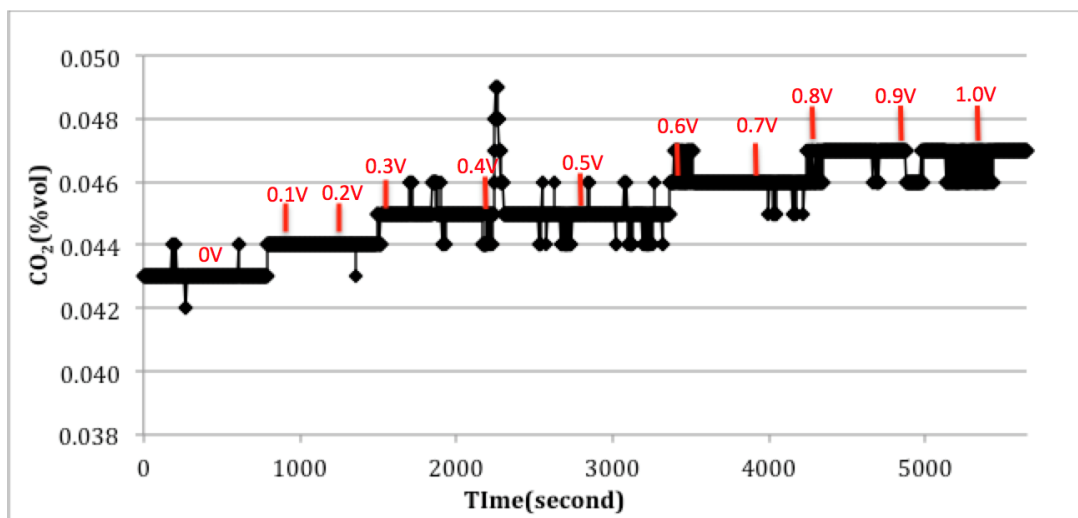
Figure 4.19 CO_2 concentration vs applied voltage at 500 °C recorded by IR
spectroscopy recorder

4.4.4 Fabrication by 'Au sputter – YSZ (O_2) thin film 8 h– Pt'

The YSZ thin film sputtered for 4 h was studied. Investigation into the issue of increased thickness of YSZ thin film has been conducted. The catalytic and electrocatalytic experiments were carried out in operating time of 8 h to assess whether it would improve the NEMCA performance.

Figure 4.20 presents the values of the faradaic efficiency vs applied voltage at 200 °C. At forward scanning, Λ increased drastically with voltage to reach a maximum value of 0.91. At higher voltage, Λ decreased gradually to a value of 0.008. The same shape of curve is obtained during reverse scanning. However, at 200 °C, Λ exhibited poor NEMCA effect but the catalytic activity and faradaic efficiency can exhibit reversible reaction from temperature at 200 °C. It is phenomenon has been studied in time of sputtering YSZ for 8 h.

From Figure 4.21, the reaction rates are constants at high voltage 0.4 – 1.0 V. during forward scanning. It shows better performance than YSZ thin film at 4 h at the same temperature which the reaction rate decreased in high voltage range 0.8 – 1.0 V. (Figure 4.16) . At 400 °C, the reaction rate is similar to the rate at high temperature 500 °C due to the thicker layer of YSZ (8 h) which response to lower temperature so well.

Figure 4.23 shows the reaction rate is enhanced electrochemically at both forward and reverse scanning. The highest ρ measured were 1.2 for forward and 1.4 for reverse scanning. Vernoux et al [59], found that on Pt, the oxidation of propane exhibits electrophobic promotion. The reaction rate was electrochemically enhanced upon application of a positive voltage. However the slight differences in the experimental conditions (between $YSZ(O_2)$ 4 h and 8 h operating time) may affect the electrochemical promotion results both, quantitatively and qualitatively. NEMCA behavior at 500 °C is similar to that of $YSZ(O_2)$ at 4 h. The reaction rate also has same trend in electrophobic type of NEMCA. The error bar was obtained indicates that it is reproducibility. To examine the type of NEMCA behavior, step change in open- and closed- circuit was experimented at forward scanning by IR spectroscopy recorder. CO_2 concentration in this case is stable as shown in Figure 4.24.
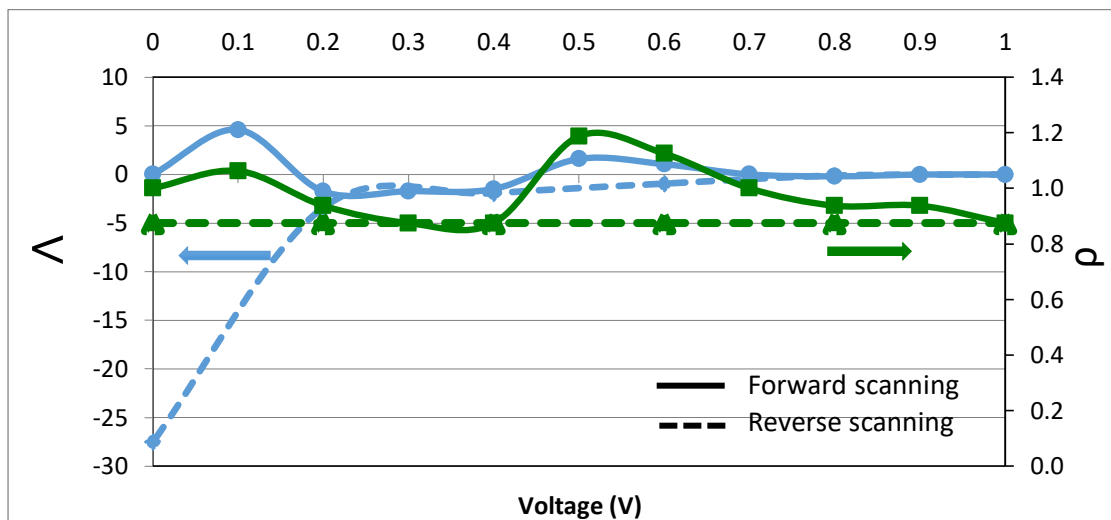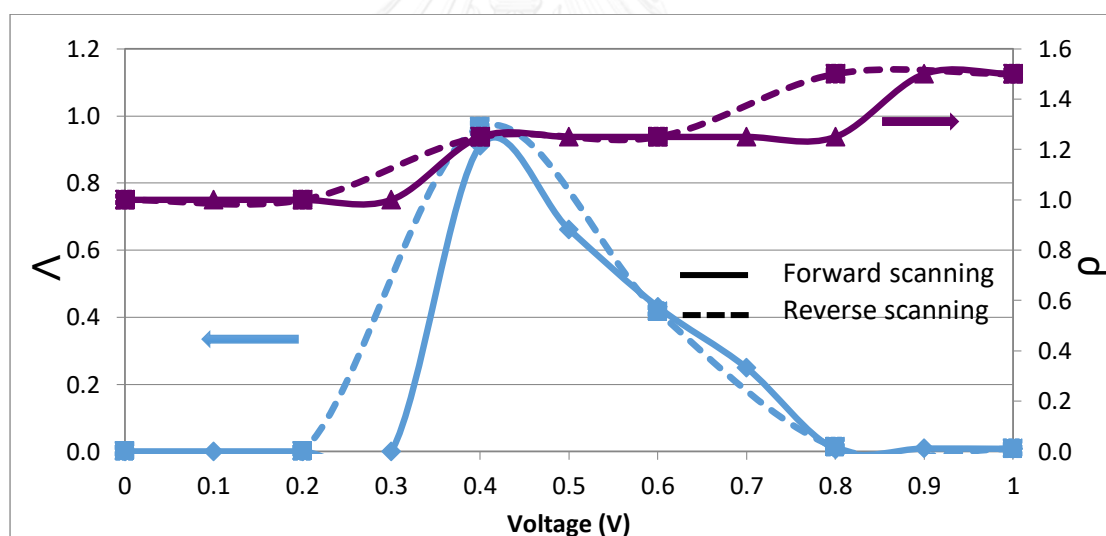

Figure 4.20 Faradaic efficiency and rate enhancement ratio vs applied voltages at 200 °C using Au sputter – $YSZ(O_2)$ thin film sputtered for 8 h – Pt
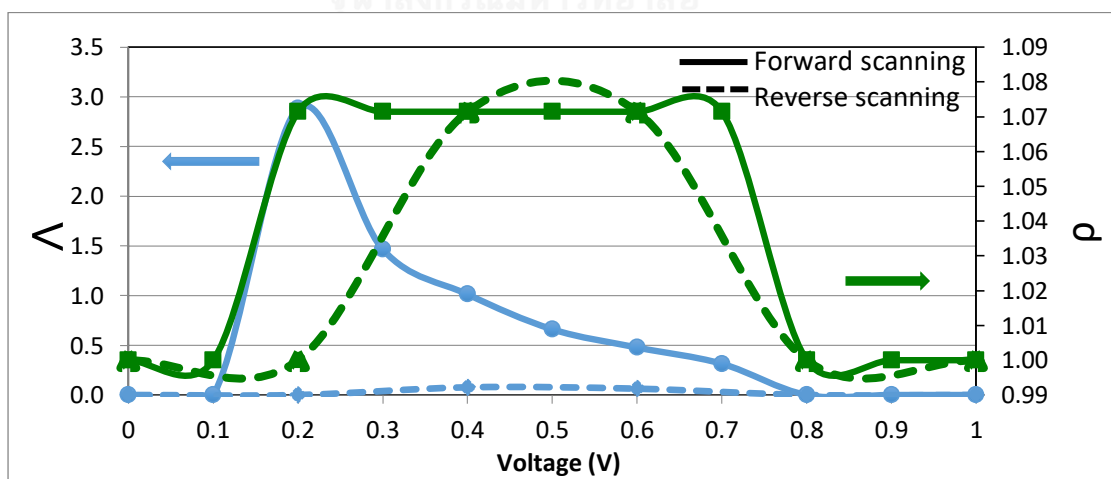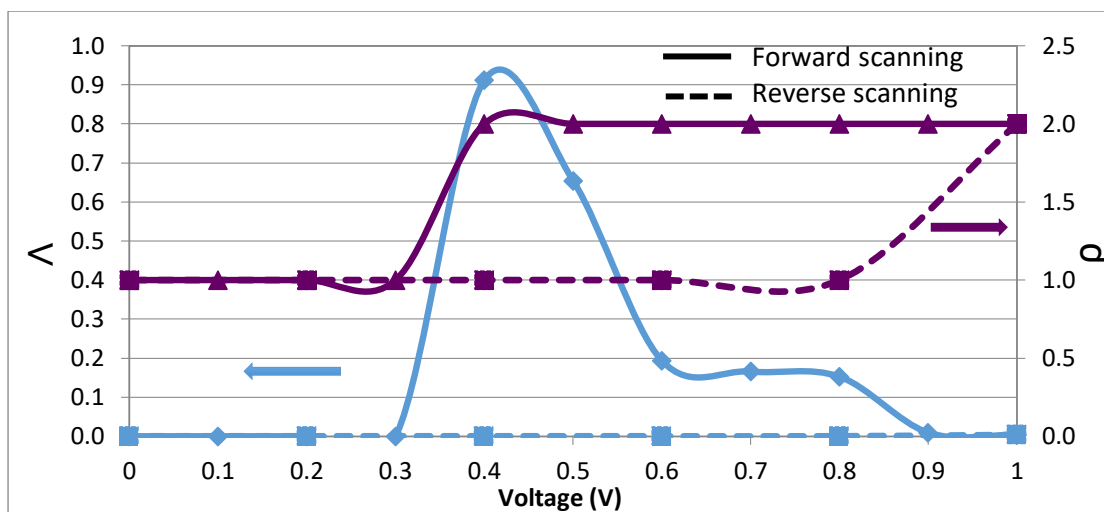
Figure 4.21 Faradaic efficiency and rate enhancement ratio vs applied voltages at 300 ˚C using Au sputter – YSZ(O$_2$) thin film sputtered for 8 h – Pt
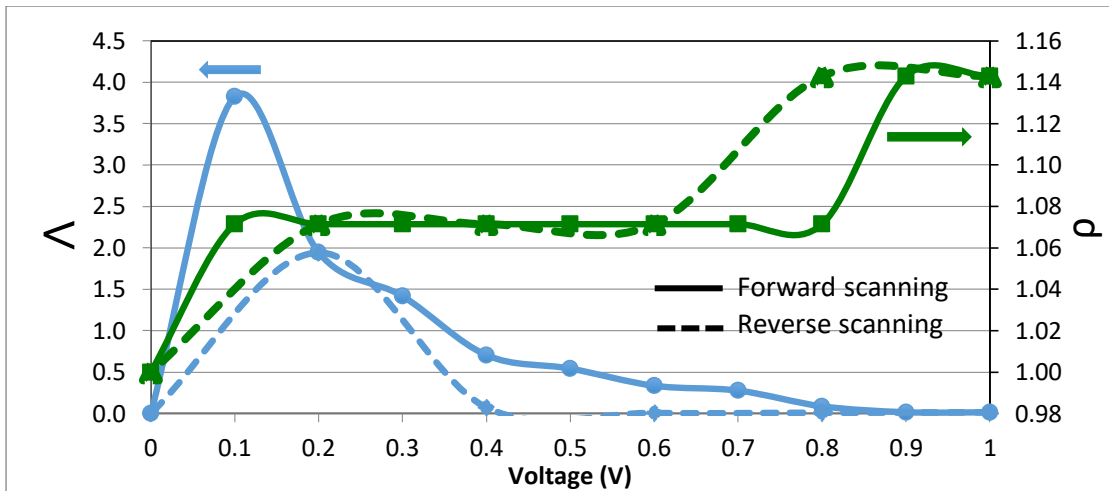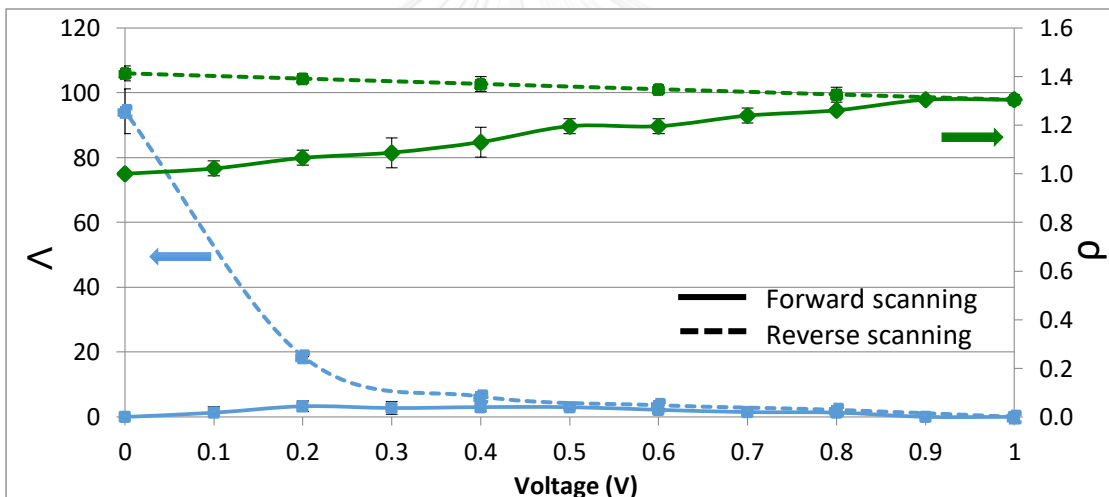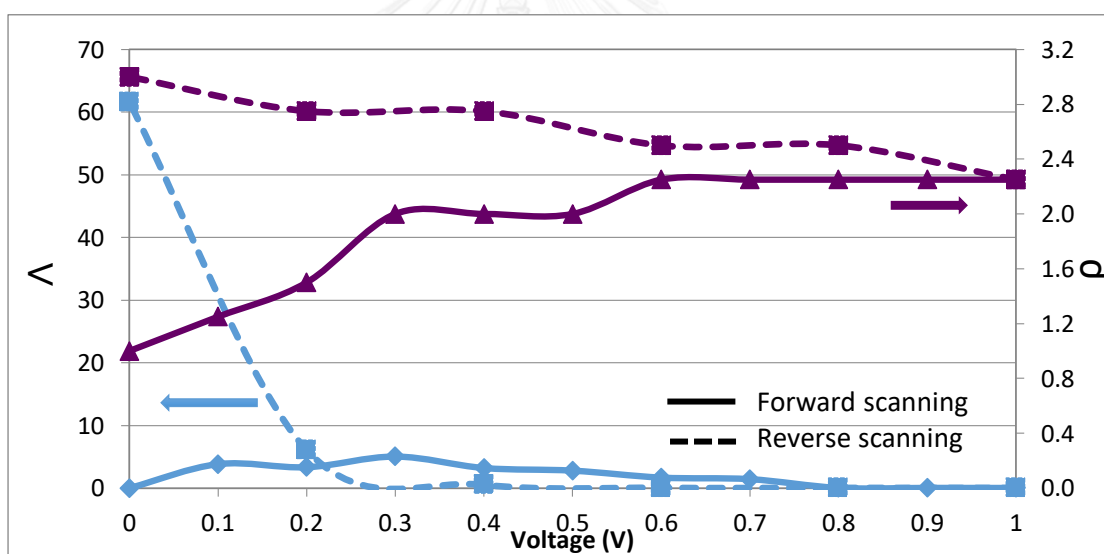

Figure 4.22 Faradaic efficiency and rate enhancement ratio vs applied voltages at 400 °C using Au sputter – YSZ(O$_2$) thin film sputtered for 8 h – Pt
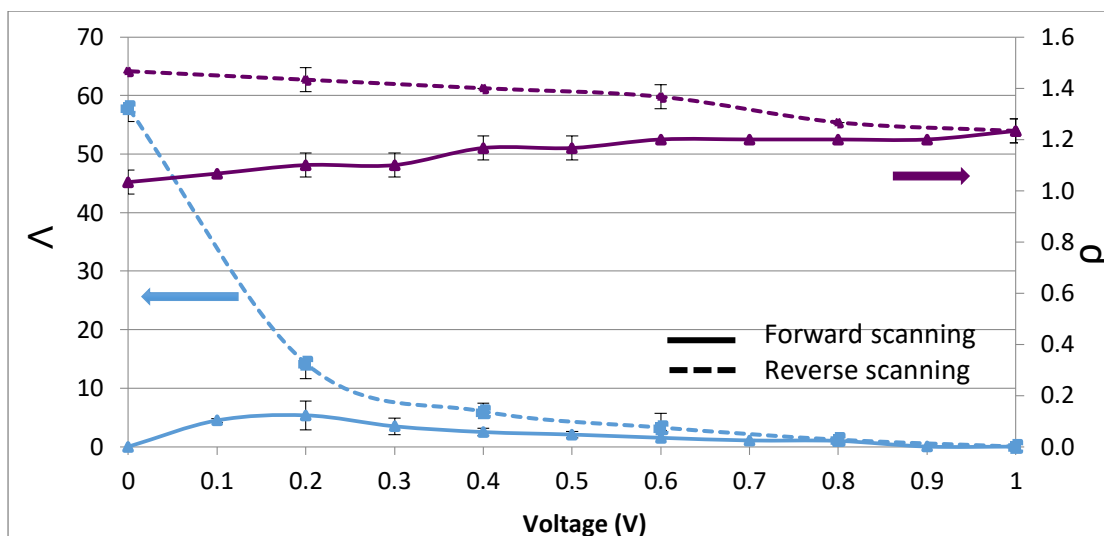
Figure 4.23 Faradaic efficiency and rate enhancement ratio vs applied voltages at 500 °C using Au sputter – $YSZ(O_2)$ thin film sputtered for 8 h – Pt
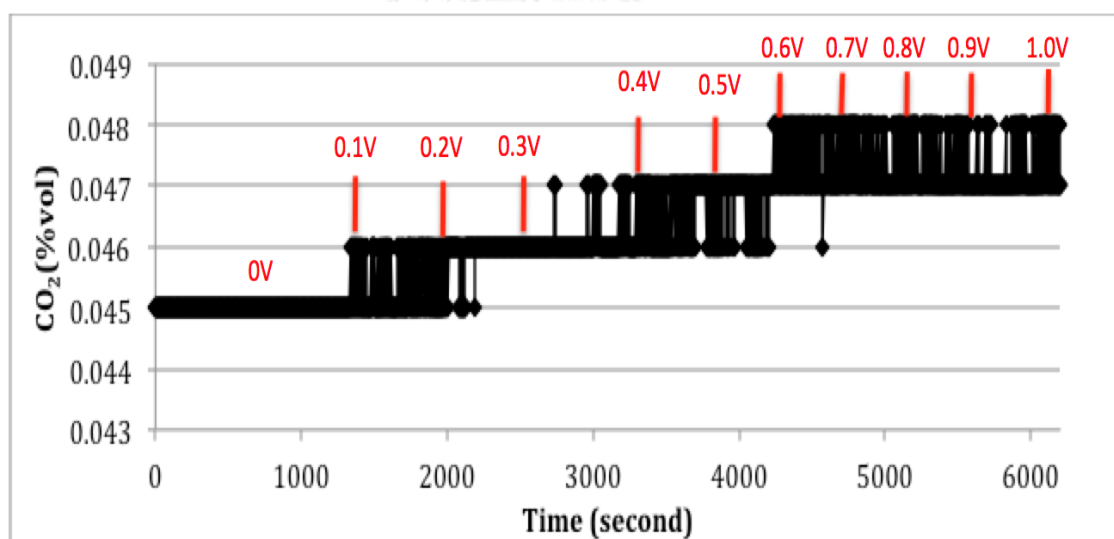
Figure 4.24 CO_2 concentration vs applied voltage at 500 °C recorded by IR spectroscopy recorder

Figure 4.25 and 4.26 present experimental data of Sareerat's project. The pellet and electrode configurations used for NEMCA was studied. A Pt catalyst film and Au film are deposited onto both sides of the YSZ disk with the thickness of 1.2 mm. The reaction was operated under the same conditions. This study shows that NEMCA can significantly affect the catalytic activity of Pt catalyst. The values of the faradaic efficiency, Λ at all temperature were examined. The forward and reverse scanning are

both reversible in either faradaic efficiency or reaction rate. In comparison, the YSZ thin film exhibited similar phenomenon especially the rate enhancement ratio at 500 °C, showing the same electrophobic behavior.
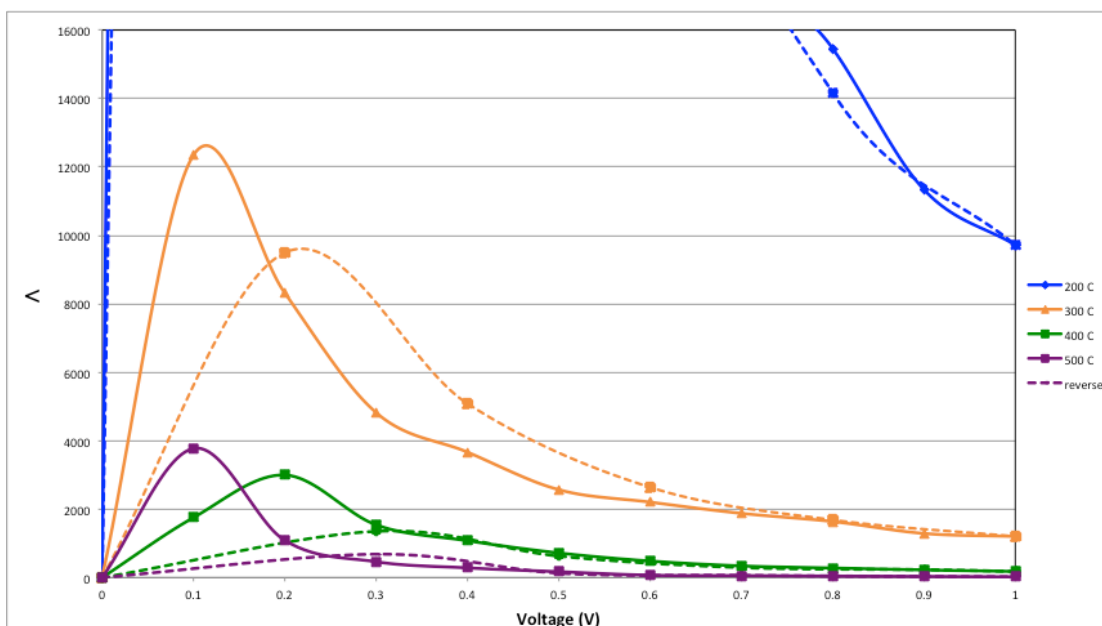
Figure 4.25 Faradaic efficiency vs applied voltages at 200-500 °C using pellet and electrode configuration [Sareerat's project].
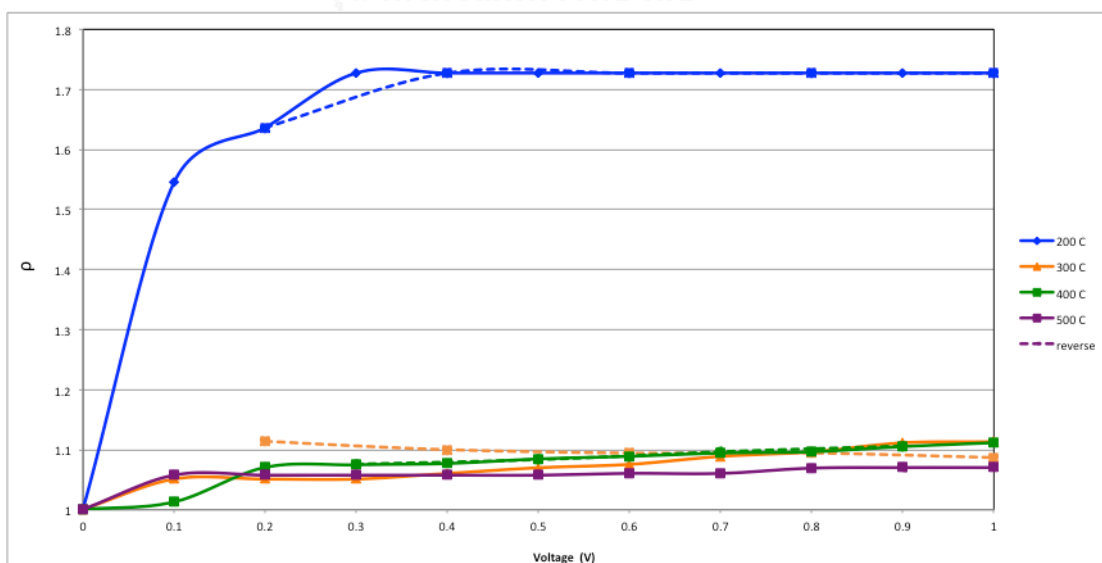
Figure 4.26 The rate enhancement ratio vs applied voltages at 200-500 °C using pellet and electrode configuration [Sareerat's project].

4.5 Propane conversion

The percentages of propane conversion increase at temperature of 500 °C and applied voltages up to 1.0 V. When YSZ(O_2) was sputtered for 4 h using operating temperature at 200 – 400 °C, the trends of propane conversion are not clear. The values present high conversion only at 500 °C. When YSZ(O_2) was sputtered for 8 h, the trends of propane conversion raised with temperature. However, the conversion at 200 °C is higher than that at 300 °C . The cause still remains undetermined, which could be a subject for future studies.
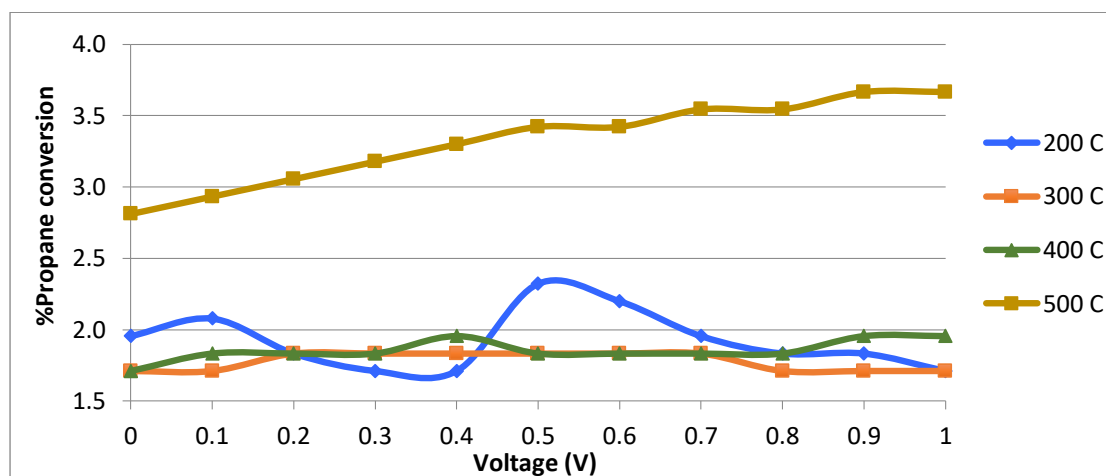
Figure 4.27 Effect of temperature and cell voltage on propane conversion with YSZ(O_2) thin film sputtered for 4 h.
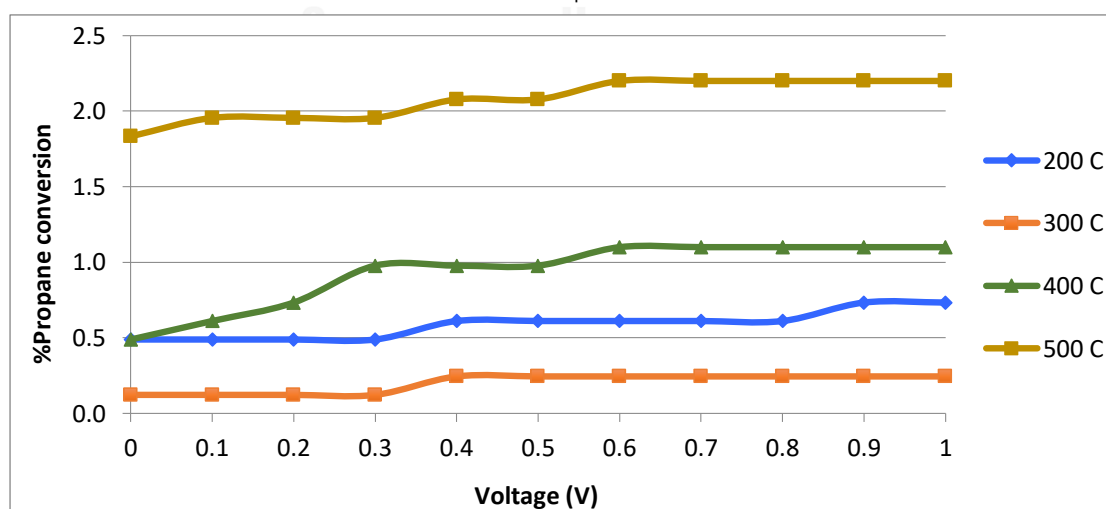
Figure 4.28 Effect of temperature and cell voltage on propane conversion with YSZ(O_2) thin film sputtered for 8 h.

4.6 Characterization of thin film electrolyte

Surface morphologies and cross sectional microstructures of the YSZ thin film on alumina substrate were investigated using scanning electron microscopy (SEM, JEOL JSM-35 CF). A more uniform film quality appeared with conventional method led to well-developed columnar grain YSZ films with uneven and rough surface morphology. However, the wireless method, there are no clear difference between YSZ thin films with alumina substrate. It appears to have clearer grain boundary in conventional condition. Crystalline structure of YSZ thin film was analyzed by X-ray diffraction (XRD, SIXMENS D5000). As indicated in XRD analysis in 2θ range between 20° to 130°. The characteristic of YSZ are observed peaks corresponding to standard JCPDS patterns for the YSZ crystal structure as shown in appendix E and F, respectively.

CHAPTER V

CONCLUSIONS AND RECOMMENDATIONS

5.1 Conclusions

The catalytic oxidation of propane on YSZ thin film on alumina substrates was studied under open-circuit and closed-circuit conditions. The cell operating by wireless method, the highest CO_2 production rate is 1.98×10^{-8} mol/s sputtering condition at 400 W for 4 h. As the cell operating by conventional method, the reaction exhibited a NEMCA effect of the electrophobic type at 500 °C with co-fed argon and oxygen gas in sputtering thin film process. Nevertheless, the catalytic activity and faradaic efficiency being reversible both of forward and reverse scanning at 400 °C for YSZ thin film is sputtered for 4 h and 200 °C for YSZ thin film is sputtered for 8 h.

5.2 Recommendations

At temperature 500 °C, the reaction rate was electrochemically enhanced both of forward and reverse scanning. In the future of work, all potentials are not necessary applied, just slight stimulate potentials. It's possible that the reaction rate still increases continuously.

Electrochemical promotion is a research issue that should explore the utilization of other catalysts, for example; non-conductive catalyst supporting material (i.e. alumina). An alternative to the catalytic process, which were affected by applied current or potentials, is based on the control work function of catalysts in order to improve the catalytic activity and product selectivity as well.

REFERENCES

[1]   Veser, G., Ziauddin, M., and Schmidt, L.D. Ignition in alkane oxidation on noble-metal catalysts. Catalysis Today 47(1-4) (1999): 219-228.

[2]   Vayenas, C., Bebelis, S., and Neophytides, S. Non-Faradaic electrochemical modification of catalytic activity. The Journal of Physical Chemistry 92(18) (1988): 5083-5085.

[3]   Yentekakis, I., Moggridge, G., Vayenas, C., and Lambert, R. In situ controlled promotion of catalyst surfaces via NEMCA: the effect of Na on the Pt-catalyzed CO oxidation. Journal of Catalysis 146(1) (1994): 292-305.

[4]   Lee, A.F., et al. The origin of SO 2 promotion of propane oxidation over Pt/Al 2 O 3 catalysts. Journal of Catalysis 184(2) (1999): 491-498.

[5]   Otto, K., Andino, J., and Parks, C. The influence of platinum concentration and particle size on the kinetics of propane oxidation over Pt/γ-alumina. Journal of Catalysis 131(1) (1991): 243-251.

[6]   Kiwi-Minsker, L., Yuranov, I., Slavinskaia, E., Zaikovskii, V., and Renken, A. Pt and Pd supported on glass fibers as effective combustion catalysts. Catalysis Today 59(1) (2000): 61-68.

[7]   Yazawa, Y., et al. The support effect on propane combustion over platinum catalyst: control of the oxidation-resistance of platinum by the acid strength of support materials. Applied Catalysis A: General 233(1) (2002): 103-112.

[8]   Steele, B. Oxygen transport and exchange in oxide ceramics. Journal of Power Sources 49(1-3) (1994): 1-14.

[9]   Steele, B.C. and Heinzel, A. Materials for fuel-cell technologies. Nature 414(6861) (2001): 345-352.

[10]   Baik, S.J., Jang, J.H., Lee, C.H., Cho, W.Y., and Lim, K.S. Highly textured and conductive undoped ZnO film using hydrogen post-treatment. Applied physics letters 70(26) (1997): 3516-3518.

[11]   Chen, X.-L., Geng, X.-H., Xue, J., and Li, L. Two-step growth of ZnO films with high conductivity and high roughness. Journal of Crystal growth 299(1) (2007): 77-81.

[12]   Yashar, P., Rechner, J., Wong, M., Sproul, W., and Barnett, S. High-rate reactive sputtering of yttria-stabilized zirconia using pulsed dc power. Surface and Coatings Technology 94 (1997): 333-338.

[13]   Delgado, J., Sánchez, F., Aguiar, R., Maniette, Y., Ferrater, C., and Varela, M. ArF and KrF excimer laser deposition of yttria-stabilized zirconia on Si (100). Applied physics letters 68(8) (1996): 1048-1050.

[14]   Kang, J.S., Kang, H.S., Pang, S.S., Shim, E.S., and Lee, S.Y. Investigation on the origin of green luminescence from laser-ablated ZnO thin film. Thin Solid Films 443(1) (2003): 5-8.

[15]   Li, T., et al. Strong green emission in ZnO films after H2 surface treatment. Journal of Physics D: Applied Physics 45(18) (2012): 185102.

[16]   Schmidt, H., Hradil, K., Hösler, W., Wersing, W., Gieres, G., and Seeböck, R. Epitaxial YBa2Cu3O x thin films on sapphire using a Y-stabilized ZrO2 buffer layer. Applied physics letters 59(2) (1991): 222-224.

[17]   Tomaszewski, H., Haemers, J., Denul, J., De Roo, N., and De Gryse, R. Yttria-stabilized zirconia thin films grown by reactive rf magnetron sputtering. Thin Solid Films 287(1) (1996): 104-109.

[18]   Pellet, C., Schwebel, C., and Hesto, P. Physical and electrical properties of yttria-stabilized zirconia epitaxial thin films deposited by ion beam sputtering on silicon. Thin Solid Films 175 (1989): 23-28.

[19]   Liu, W., et al. Structure, luminescence and electrical properties of ZnO thin films annealed in H 2 and H 2 O ambient: A comparative study. Thin Solid Films 518(14) (2010): 3923-3928.

[20]   Natsume, Y. and Sakata, H. Electrical and optical properties of zinc oxide films post-annealed in H 2 after fabrication by sol–gel process. Materials Chemistry and Physics 78(1) (2003): 170-176.

[21]   Yentekakis, I.V., Moggridge, G., Vayenas, C.G., and Lambert, R.M. In-Situ Controlled Promotion of Catalyst Surfaces Via Nemca - the Effect of Na on the Pt-Catalyzed Co Oxidation. <u>Journal of Catalysis</u> 146(1) (1994): 292-305.

[22]   Tsiplakides, D., Neophytides, S.G., Enea, O., Jaksic, M., and Vayenas, C.G. Nonfaradaic electrochemical modification of the catalytic activity of Pt-black electrodes deposited on nafion 117 solid polymer electrolytes. <u>Journal of the Electrochemical Society</u> 144(6) (1997): 2072-2078.

[23]   Vayenas, C.G., Brosda, S., and Pliangos, C. Rules and mathematical modeling of electrochemical and chemical promotion 1. Reaction classification promotional rules. <u>Journal of Catalysis</u> 203(2) (2001): 329-350.

[24]   Souentie, S., Lizarraga, L., Papaioannou, E.I., Vayenas, C.G., and Vernoux, P. Permanent electrochemical promotion of C3H8 oxidation over thin sputtered Pt films. <u>Electrochemistry Communications</u> 12(8) (2010): 1133-1135.

[25]   Lizarraga, L., Guth, M., Billard, A., and Vernoux, P. Electrochemical catalysis for propane combustion using nanometric sputtered-deposited Pt films. <u>Catalysis Today</u> 157(1-4) (2010): 61-65.

[26]   Tsampas, M.N., Sapountzi, F.M., and Vernoux, P. Applications of yttria stabilized zirconia (YSZ) in catalysis. <u>Catalysis Science & Technology</u> 5(11) (2015): 4884-4900.

[27]   Chen, M., Hallstedt, B., and Gauckler, L.J. Thermodynamic modeling of the ZrO2-YO1.5 system. <u>Solid State Ionics</u> 170(3-4) (2004): 255-274.

[28]   Baumard, J., Heuer, P.A.A., and Hobbs, L. Advances in Ceramics, Vol. 3. <u>Science and Technology of Zirconia II, American Ceramic Society, Columbus, OH</u> (1981): 555.

[29]   Su, Y.J. <u>Processing and performance of yttrium-stabilized zirconia-based multilayer thermal barrier coatings</u>. 2001.

[30]   Minh, N.Q. Solid oxide fuel cell technology—features and applications. <u>Solid State Ionics</u> 174(1) (2004): 271-277.

[31]   Chour, K.W., Chen, J., and Xu, R. Metal-organic vapor deposition of YSZ electrolyte layers for solid oxide fuel cell applications. <u>Thin Solid Films</u> 304(1-2) (1997): 106-112.

[32]   Charpentier, P., Fragnaud, P., Schleich, D.M., and Gehain, E. Preparation of thin film SOFCs working at reduced temperature. <u>Solid State Ionics</u> 135(1-4) (2000): 373-380.

[33]   Jang, W.S., Hyun, S.H., and Kim, S.G. Preparation of YSZ/YDC and YSZ/GDC composite electrolytes by the tape casting and sol-gel dip-drawing coating method for low-temperature SOFC. <u>Journal of Materials Science</u> 37(12) (2002): 2535-2541.

[34]   Wang, J., Yan, D., Pu, J., Chi, B., and Jian, L. Fabrication and performance evaluation of planar solid oxide fuel cell with large active reaction area. <u>International Journal of Hydrogen Energy</u> 36(12) (2011): 7234-7239.

[35]   Rotureau, D., Viricelle, J.P., Pijolat, C., Caillol, N., and Pijolat, M. Development of a planar SOFC device using screen-printing technology. <u>Journal of the European Ceramic Society</u> 25(12) (2005): 2633-2636.

[36]   Chang, Y.C., et al. Characterization of Anode-Supported Solid Oxide Fuel Cells with Composite LSM-YSZ and LSM-GDC Cathodes. <u>Journal of the Electrochemical Society</u> 158(3) (2011): B259-B265.

[37]   Wong, M.S., Chia, W.J., Yashar, P., Schneider, J.M., Sproul, W.D., and Barnett, S.A. High-rate reactive dc magnetron sputtering of ZrOx coatings. <u>Surface & Coatings Technology</u> 86(1-3) (1996): 381-387.

[38]   Kinder, H., Berberich, P., Utz, B., and Prusseit, W. Double sided YBCO films on 4" substrates by thermal reactive evaporation. <u>IEEE Transactions on Applied Superconductivity</u> 5(2) (1995): 1575-1580.

[39]   Fu, C.J., Chan, S.H., Liu, Q.L., Ge, X.M., and Pasciak, G. Fabrication and evaluation of Ni-GDC composite anode prepared by aqueous-based tape casting method for low-temperature solid oxide fuel cell. <u>International Journal of Hydrogen Energy</u> 35(1) (2010): 301-307.

[40]   Smeacetto, F., et al. Yttria-stabilized zirconia thin film electrolyte produced by RF sputtering for solid oxide fuel cell applications. <u>Materials Letters</u> 64(22) (2010): 2450-2453.

[41]   Hong, S., Yang, H., Lim, Y., and Kim, Y.B. Microstructure-controlled deposition of yttria-stabilized zirconia electrolyte for low temperature solid oxide fuel cell performance stability enhancement. Thin Solid Films 618 (2016): 207-212.

[42]   Jankowski, A.F. and Hayes, J.P. Reactive sputter deposition of yttria-stabilized zirconia. Surface & Coatings Technology 76(1-3) (1995): 126-131.

[43]   Park, Y.-i., Saito, Y., Pornprasertsuk, R., Cheng, J., Cha, S.-w., and Prinz, F.B. Electrical properties of YSZ thin films deposited on nanoporous substrates. in Electrochem. Soc. Proc., pp. 169-180, 2003.

[44]   Liu, B.X., Zhang, Z.J., and Jin, O. A comparative study of metastable alloy formation by ion mixing and thermal annealing of multilayers in the immiscible Y-Zr system. Journal of Alloys and Compounds 270(1-2) (1998): 186-193.

[45]   Scott, H. Phase relationships in the zirconia-yttria system. Journal of Materials Science 10(9) (1975): 1527-1535.

[46]   Vayenas, C.G. and Bebelis, S. Electrochemical promotion of heterogeneons catalysis. Catalysis Today 51(3-4) (1999): 581-594.

[47]   Vayenas, C.G. and Bebelis, S.I. Electrochemical promotion. Solid State Ionics 94(1-4) (1997): 267-277.

[48]   Vayenas, C.G., et al. Electrochemical Promotion in Catalysis - Non-Faradaic Electrochemical Modification of Catalytic Activity. Electrochimica Acta 39(11-12) (1994): 1849-1855.

[49]   Bebelis, S., Karasali, H., and Vayenas, C.G. Electrochemical promotion of the CO2 hydrogenation on Pd/YSZ and Pd/beta "-Al2O3 catalyst-electrodes. Solid State Ionics 179(27-32) (2008): 1391-1395.

[50]   Bebelis, S., Karasali, H., and Vayenas, C.G. Electrochemical promotion of CO(2) hydrogenation on Rh/YSZ electrodes. Journal of Applied Electrochemistry 38(8) (2008): 1127-1133.

[51]   Frantzis, A.D., Bebelis, S., and Vayenas, C.G. Electrochemical promotion (NEMCA) of CH4 and C2H4 oxidation on Pd/YSZ and investigation of the origin of NEMCA via AC impedance spectroscopy. Solid State Ionics 136 (2000): 863-872.

[52]   Giannikos, A., Frantzis, A.D., Pliangos, C., Bebelis, S., and Vayenas, C.G. Electrochemical Promotion of CH(4) Oxidation on Pd. Ionics 4(1-2) (1998): 53-60.

[53]   Jimenez-Borja, C., Delgado, B., Diaz-Diaz, L.F., Valverde, J.L., and Dorado, F. Enhancing the combustion of natural gas by electrochemical promotion of catalysis. Electrochemistry Communications 23 (2012): 9-12.

[54]   Bebelis, S. and Kotsionopoulos, N. Non-faradaic electrochemical modification of the catalytic activity for propane combustion of Pt/YSZ and Rh/YSZ catalyst-electrodes. Solid State Ionics 177(26-32) (2006): 2205-2209.

[55]   Tsiakaras, P. and Vayenas, C.G. Non-Faradaic Electrochemical Modification of Catalytic Activity .12. The Case of Methane Oxidation on Platinum. Journal of Catalysis 140(1) (1993): 53-70.

[56]   Marwood, M. and Vayenas, C.G. Electrochemical promotion of a dispersed platinum catalyst. Journal of Catalysis 178(2) (1998): 429-440.

[57]   Kaloyannis, A. and Vayenas, C.G. Non-faradaic electrochemical modification of catalytic activity .11. Ethane oxidation on Pt. Journal of Catalysis 171(1) (1997): 148-159.

[58]   Kaloyannis, A. and Vayenas, C.G. Non-Faradaic electrochemical modification of catalytic activity - 12. Propylene oxidation on Pt. Journal of Catalysis 182(1) (1999): 37-47.

[59]   Vernoux, P., Gaillard, F., Bultel, L., Siebert, E., and Primet, M. Electrochemical promotion of propane and propene oxidation on Pt/YSZ. Journal of Catalysis 208(2) (2002): 412-421.

[60]   Marwood, M. and Vayenas, C.G. Electrochemical promotion of electronically isolated Pt catalysts on stabilized zirconia. Journal of Catalysis 168(2) (1997): 538-542.

[61]   Tsampas, M.N. and Vernoux, P. New and Future Developments in Catalysis: Chapter 11. Electrochemical Promotion of Catalysis for Automotive Post-Treatment and Air Cleaning. Elsevier Inc. Chapters, 2013.

[62]   Akasaka, S. Thin film YSZ-based limiting current-type oxygen and humidity sensor on thermally oxidized silicon substrates. <u>Sensors and Actuators B-Chemical</u> 236 (2016): 499-505.

[63]   Hong, S.W., Lee, D.H., Lim, Y.H., Bae, J.W., and Kim, Y.B. Yttria-stabilized zirconia thin films with restrained columnar grains for oxygen ion conducting electrolytes. <u>Ceramics International</u> 42(15) (2016): 16703-16709.

[64]   Marwood, M. and Vayenas, C. Electrochemical promotion of electronically isolated Pt catalysts on stabilized zirconia. <u>Journal of Catalysis</u> 168(2) (1997): 538-542.

[65]   Bockris, J., Conway, B., and White, R. <u>Modern aspects of electrochemistry Vol. 29</u>. Springer, 1995.

[66]   Kokkofitis, C., Karagiannakis, G., Zisekas, S., and Stoukides, M. Catalytic study and electrochemical promotion of propane oxidation on Pt/YSZ. <u>Journal of Catalysis</u> 234(2) (2005): 476-487.

[67]   Vayenas, C.G. <u>Electrochemical activation of catalysis: promotion, electrochemical promotion, and metal-support interactions</u>. Springer Science & Business Media, 2001.

[68]   Rahul, S., Balasubramanian, K., and Venkatesh, S. Inkjet Printing of 5 Mol% YSZ Nano Particle Suspensions on Porous α-Al2O3 Substrates. <u>Materials Today: Proceedings</u> 2(4-5) (2015): 3552-3564.

[69]   Jankowski, A. and Hayes, J. Reactive sputter deposition of yttria-stabilized zirconia. <u>Surface and coatings technology</u> 76 (1995): 126-131.

APPENDIX

APPENDIX A

YSZ THIN FILM BY SCREEN PRINTING METHOD

Screen-printing technology was developed to fabricate dense YSZ electrolyte film on alumina substrate. To reduce the cost of fabrication. YSZ powder was mixed with appropriate organic vehicles to make homogeneous and printing inks. The ink was extruded through a screen onto the substrate by scraping blade. Finally, the substrate with printed electrolyte film was dried and co-fired at high temperature to densify the YSZ film. The screen-printing technique is cost-effective and simple. This is the great commercial interest due to low-cost and high availability of such equipment on the market.

- Printing ink preparation

YSZ particles and organic vehicle were used to prepare the printing ink. The organic vehicle contains ethylcellulose and terpineol as a binder and a plasticizer, respectively. Binders are intended primarily for good adhesion with the substrates[68]. YSZ and the organic vehicle (6 wt% ethylcellulose and 94% terpineol) were mixed in an agate mortar at a ratio of 60:40, 40:60 and 70:30 and ground to get a homogeneous paste.

YSZ printing ink was screen printed though a screen mesh of 120 wires cm^{-1} onto alumina disks by a rubber squeegee. The distance between the screen and the top surface of substrate was 5 mm. The wet YSZ-alumina pellets were dried in air and sintered at 1200 °C for 4 h at a heating rate of 5 °C/min to densify the YSZ films.

The effect of YSZ content on the CO_2 production rates was tested and the results were plotted in Figure A.1-A.3 . The viscosity of the printing ink increases with increasing YSZ content. The reaction rate of CO_2 increased from 1.61×10^{-10} to 3.55×10^{-9} mol s^{-1} at 60wt% YSZ , from 4.84×10^{-10} to 2.58×10^{-9} mol s^{-1} at 40wt% YSZ and

from 2.42×10^{-9} to 1.03×10^{-7} mol s^{-1} at 70wt% YSZ as the temperature increase from 200 to 550 °C and the maximum rate enhancement ratios were 2, 1.33 and 1.33 at 60wt% , 40wt% and 70wt%, respectively. (FigureA.1 –A.3)
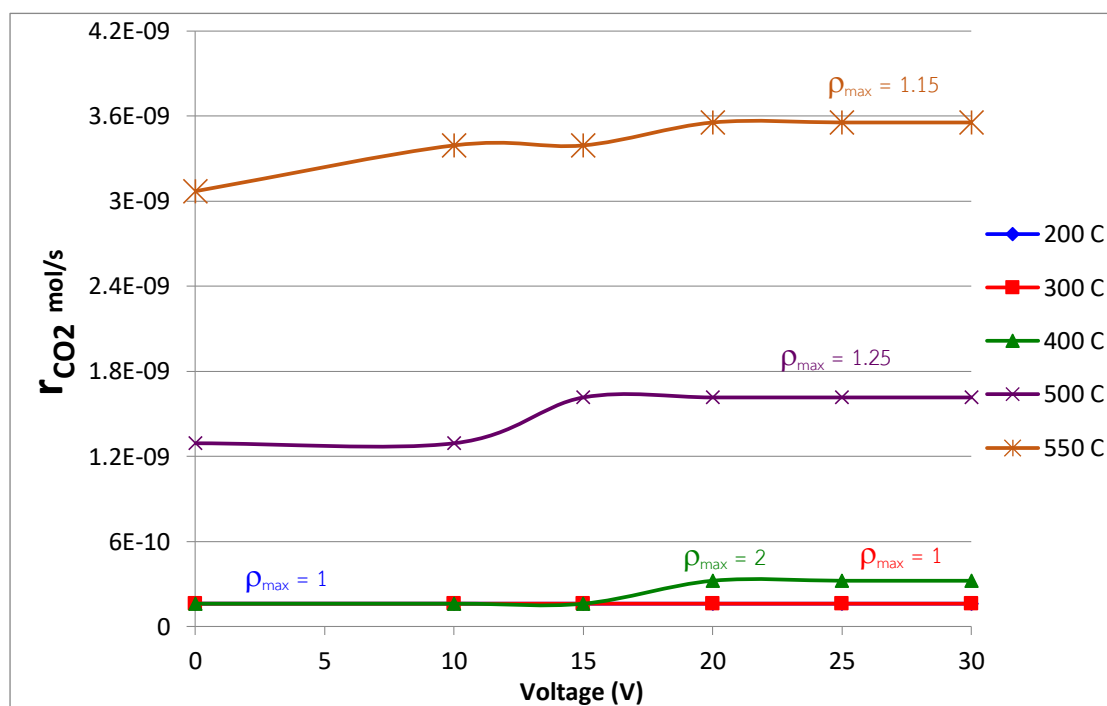

Figure A.1 Effect of the applied potential and temperature on the electrochemically promoted propane oxidation on Pt catalyst deposited on YSZ thin films prepared by screen printing at 60wt% YSZ
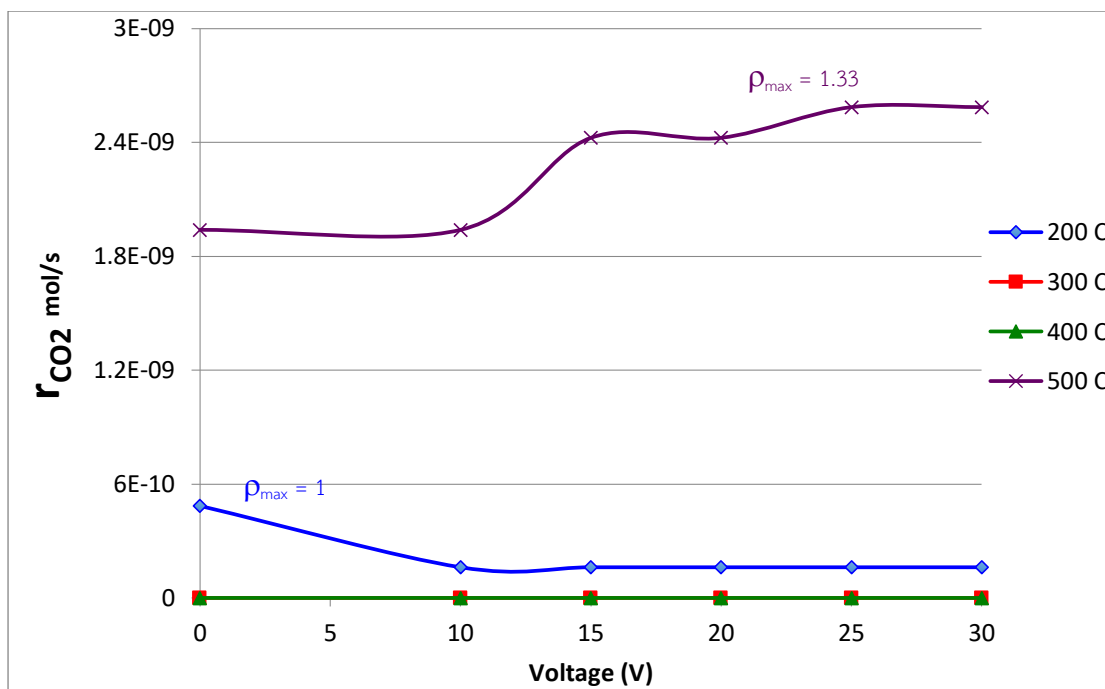
Figure A.2 Effect of the applied potential and temperature on the electrochemically promoted propane oxidation on Pt catalyst deposited on YSZ thin films prepared by screen printing at 40wt% YSZ
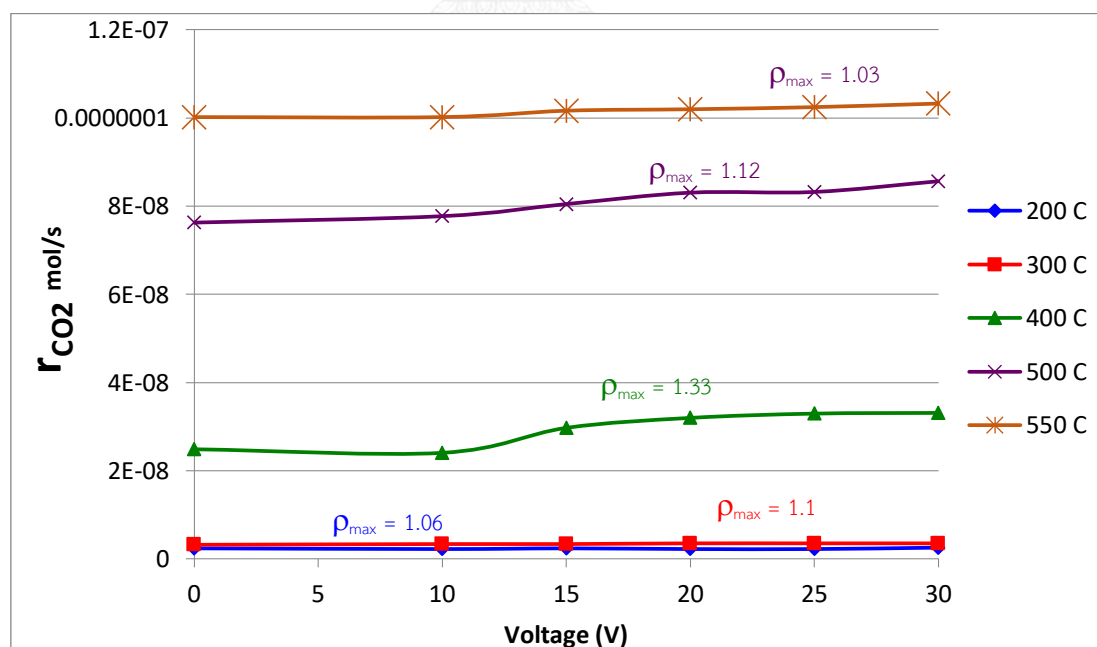

Figure A.3 Effect of the applied potential and temperature on the electrochemically promoted propane oxidation on Pt catalyst deposited on YSZ thin films prepared by screen printing at 70wt% YSZ

From experiment screen-printing technique by wireless method can not found current data same sputtering technique result in can not obtained faradaic efficiency parameter. The rate of CO_2 and the rate enhancement ratios were carried out in each temperature. To improve the cell reaction, conventional method was investigated by screen printing technique. The limitation of Au electrode can not available at high temperature. Therefore, Pt electrode was used as counter and working electrode. The faradaic efficiency was obtained. The cell response at 5 V and 10 V of potentials that increase for a while until high potentials is reached, decrease in $\wedge$ is observed. (Figure A.4)
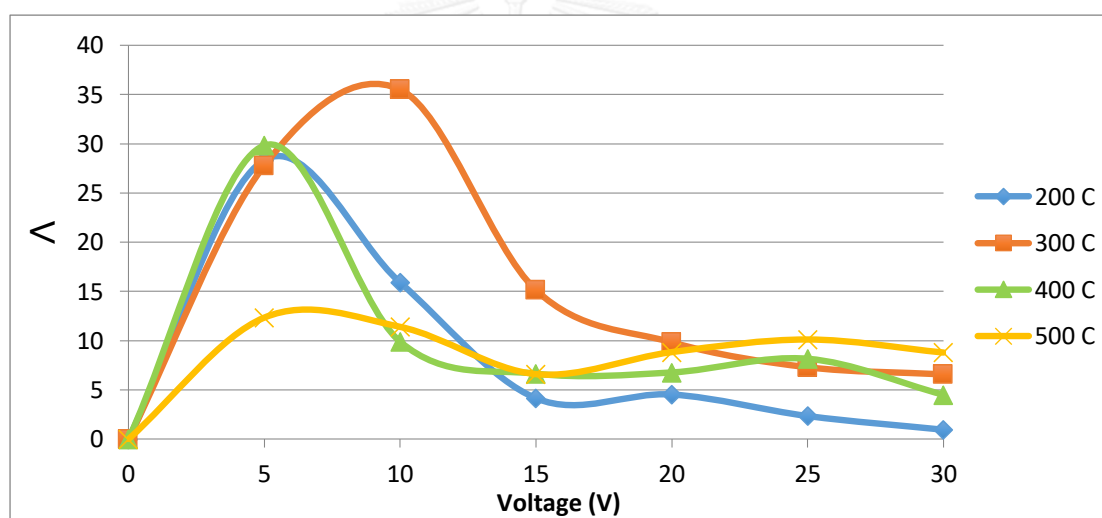

Figure A.4 Faradaic efficiency on applied voltages at 200-500 °C by Pt – YSZ – Pt by screen-printing technique

- Microstructure of YSZ thin films

The viscosity of the printing ink is very important for screen printing. The viscosity of ink can be controlled by adjusting the ratio of the YSZ powder to the organic vehicle. If the YSZ content is too low, a porous film is observed because of the volatilation of the during sintering of the film. If the YSZ content is too high, cracks are observed because of the poor rheology of the ink as shown in Figure A.5 and Figure A.6.
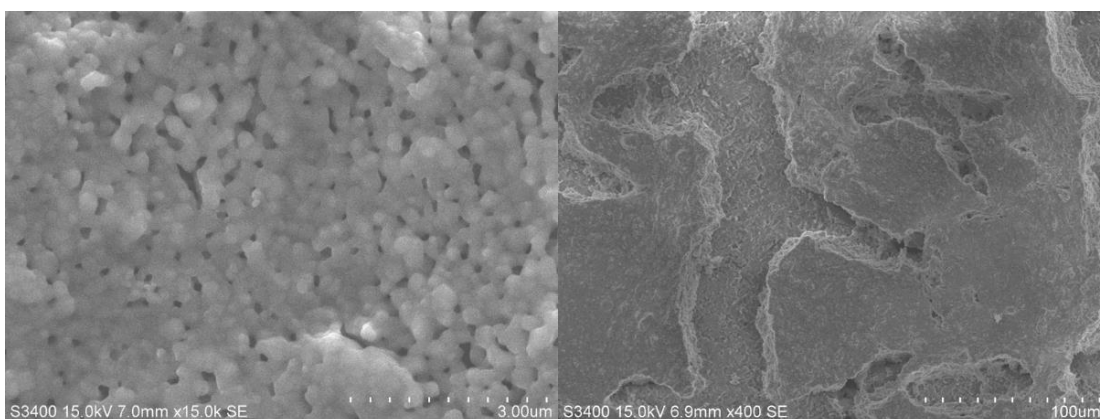
Figure A.5 Surface microstructure of screen-printed YSZ films at YSZ content 60 wt%
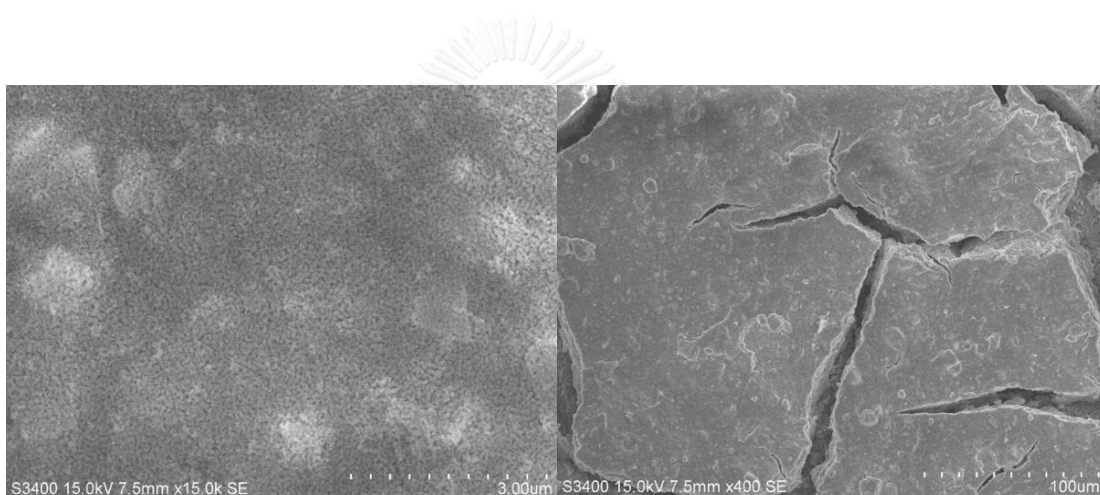

Figure A.6 Surface microstructure of screen-printed YSZ films at YSZ content 70 wt%

Table A.1 shows elemental analysis of yttria and zirconia in at%. At YSZ content of 70 wt%, the ratio is closer to 8 mol% yttria-stabilized zirconia, which yields the optimum oxygen-ion conductivity for cubic YSZ at elevated temperatures[69] and exhibits a nanocrystalline structure of $Zr_{.85}Y_{.15}O_{1.93}$ (fcc)[40].

Table A.1 Surface elemental composition of screen-printed YSZ films.

Element	YSZ content	
	60 wt%	70 wt%
Y (at%)	16.45	15.42
Zr (at%)	83.55	84.28

APPENDIX B

CALCULATION FOR CATALYST PREPARATION

Preparation of catalyst for wireless method

The chemical used for all the catalysts preparation

- Chloropaltinic acid (38% Pt), Aldrich

- Wet impregnation (WI)

From BET surface area of YSZ powder = 58.5749 m^2 g^{-1} = 58.5749x10^4 cm^2 g^{-1}

From ICP Pt on YSZ = 239.6 mg L^{-1}

Surface area of Alumina disk = 1.912 cm^2

Surface loading of platinum = $\dfrac{\mathbf{239.6 \times 10^{-3}\ g\ L^{-1}}}{\mathbf{(17.072\ g\ L^{-1}) \times (58.5749 \times 10^4 cm^2 g^{-1})}}$

= 2.396 x 10^{-8} g Pt cm^{-2}

Then, Surface area of Alumina disk 1.912 cm^2;

Required platinum   = 1.912 cm^2 x 2.396 x 10^{-8} g cm^{-2}

= 4.58 x 10^{-8} g of Pt

Therefore, Chloroplatinic acid required in grams = $\dfrac{100g \times 4.58 \times 10^{-8} g}{38\ g}$

= 1.205 x 10^{-7} g

APPENDIX C

CALCULATION FOR THE RATE ENHANCEMENT RATIO AND FARADAIC EFFICIENCY

Propane oxidation : $C_3H_8 + 5O_2$ → $3CO_2 + 4H_2O$

Electrochemical propane oxidation : $C_3H_8 + 10O^{2-}$ → $20e^- + 3CO_2 + 4H_2O$
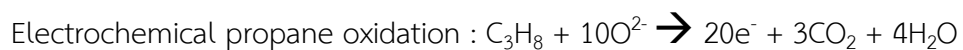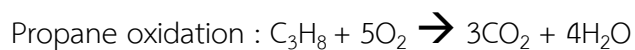
The rate enhancement ratio, ρ

$$\rho = \frac{r}{r_0}$$

Where r = the electrochemically promoted catalytic rate

r_0 = the catalytic rate at open circuit

The faradaic efficiency, Λ

$$\Lambda = \frac{(r - r_0)}{(I/nF)}$$

where I is the applied current

n is the charge of the promotion ion

F is Faraday's constant (96485 C mol^{-1})

For example,

Feed gas C_3H_8 16.67 cm^3/min, O_2 33.33 cm3/min, He 50 cm^3/min

No catalyst (blank) obtained CO_2 concentration = 0.03 vol%

At open circuit obtain CO_2 concentration = 0.38 vol%

At 500°C, 0.1 V. obtain CO_2 concentration = 0.4 vol% and current 1.09×10^{-4} A.

(1.09×10^{-4} C/s)

$$r = \frac{1}{3} \times \frac{\frac{(0.4-0.03)}{100} \times (16.67+33.33+50)cm^3min^{-1} \times \frac{1\,min}{60\,s} \times 10^5 Pa}{8314000\ cm^3\ Pa\ K^{-1}mol^{-1} \times (30+273.15)K}$$

$$= 8.16 \times 10^{-8}$$

$$r_0 = \frac{1}{3} \times \frac{\frac{(0.38-0.03)}{100} \times (16.67+33.33+50)cm^3min^{-1} \times \frac{1\,min}{60\,s} \times 10^5 Pa}{8314000\ cm^3\ Pa\ K^{-1}mol^{-1} \times (30+273.15)K}$$

$$= 7.72 \times 10^{-8}$$

So, $\Lambda = \dfrac{(r-r_0)}{(I/nF)} = \dfrac{(8.16 \times 10^{-8} - 7.72 \times 10^{-8}\,mol\,s^{-1})}{1.09 \times 10^{-4}\ Cs^{-1}/(20 \times 96485\ Cmol^{-1})} = 78.03$

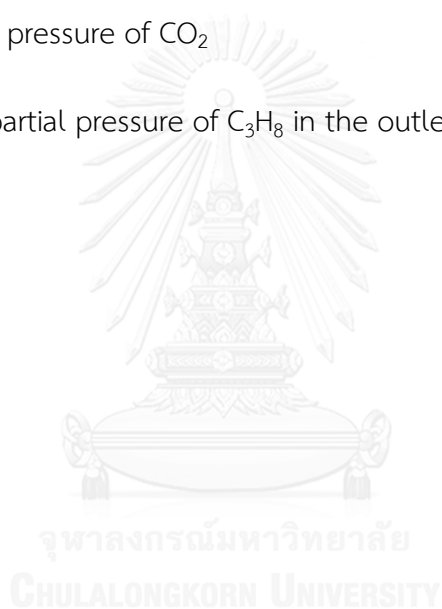$$\rho = \frac{r}{r_0} = \frac{8.16 x 10^{-8}}{7.72 x 10^{-8}} = 1.057$$

APPENDIX D

CALCULATION FOR METAL FOR PROPANE OXIDATION

Propane oxidation: $C_3H_8 + 5O_2 \rightarrow 3CO_2 + 4H_2O$
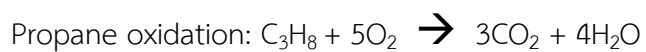
The propane conversion was calculated $= \dfrac{P_{CO_2}}{P_{CO_2} + 3P_{C_3H_8}} \times 100\%$

Where P_{CO_2} are partial pressure of CO_2

P_{C3H8} are the partial pressure of C_3H_8 in the outlet gas

APPENDIX E

THE CHARACTERIZATION CATALYST BY SEM - EDX TECHNIQUE

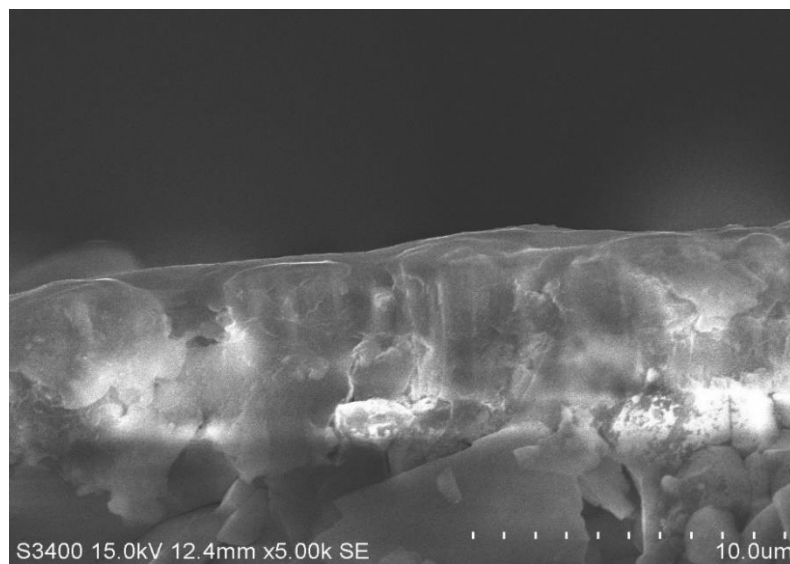The cross-sectional morphologies of the fabricated YSZ thin film sample were observed using SEM.

Figure E.1 SEM image of the cross sectional view of YSZ thin film deposited on alumina using wireless method: 400 W for 4 h
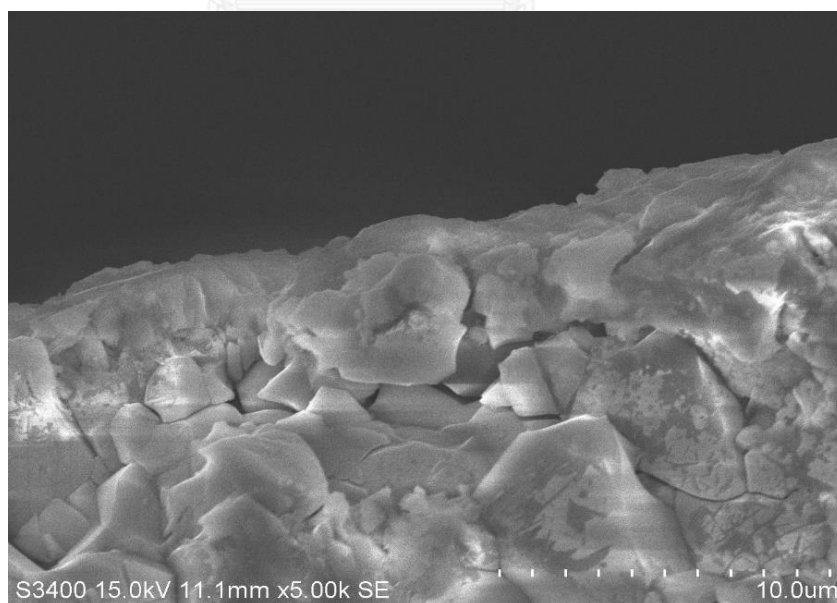

Figure E.2 SEM image of the cross sectional view of YSZ thin film deposited on alumina using wireless method: 200 W for 4 h
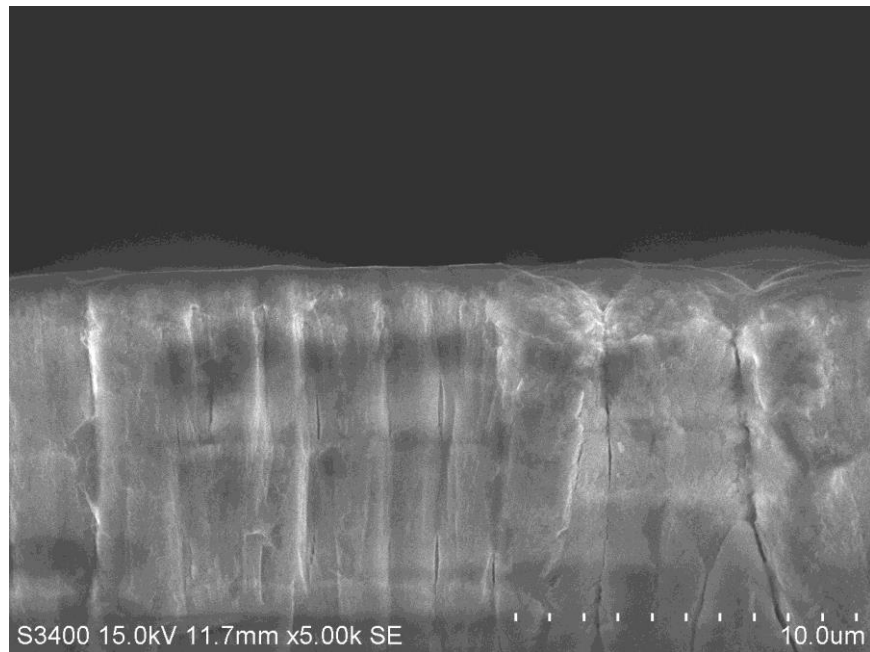
Figure E.3 SEM image of the cross sectional view of YSZ thin film deposited on alumina using wireless method: 200 W for 8 h
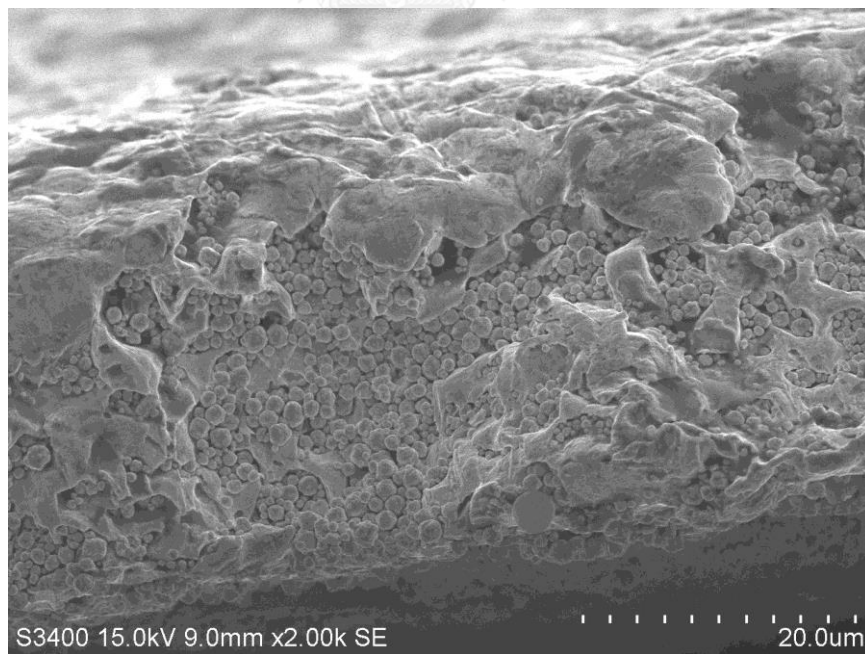

Figure E.4 SEM image of the cross sectional view of YSZ thin film deposited on alumina using conventional method: Au paste – YSZ(O_2) - Pt
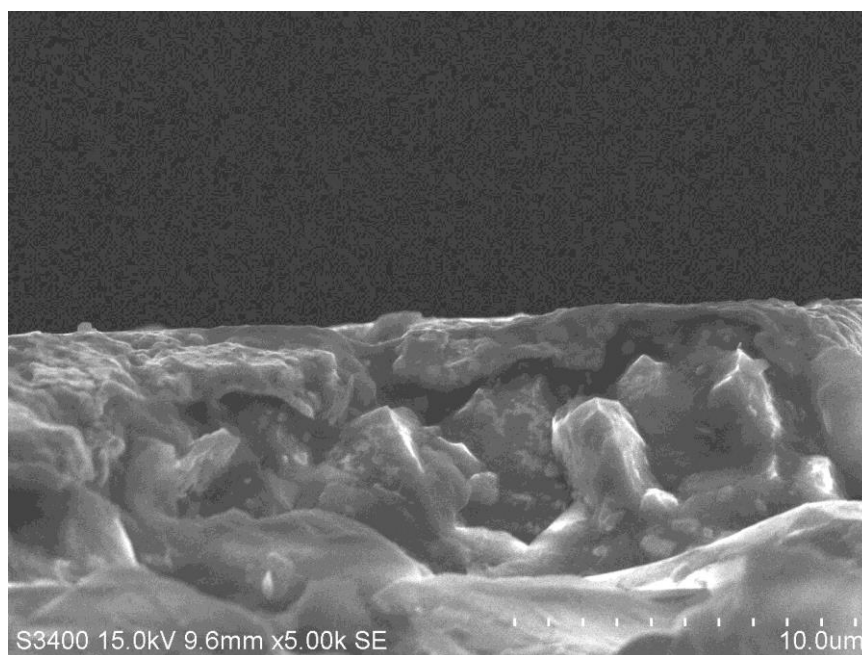
Figure E.5 SEM image of the cross sectional view of YSZ thin film deposited on alumina using conventional method: Au sputter – YSZ(O$_2$) - Pt
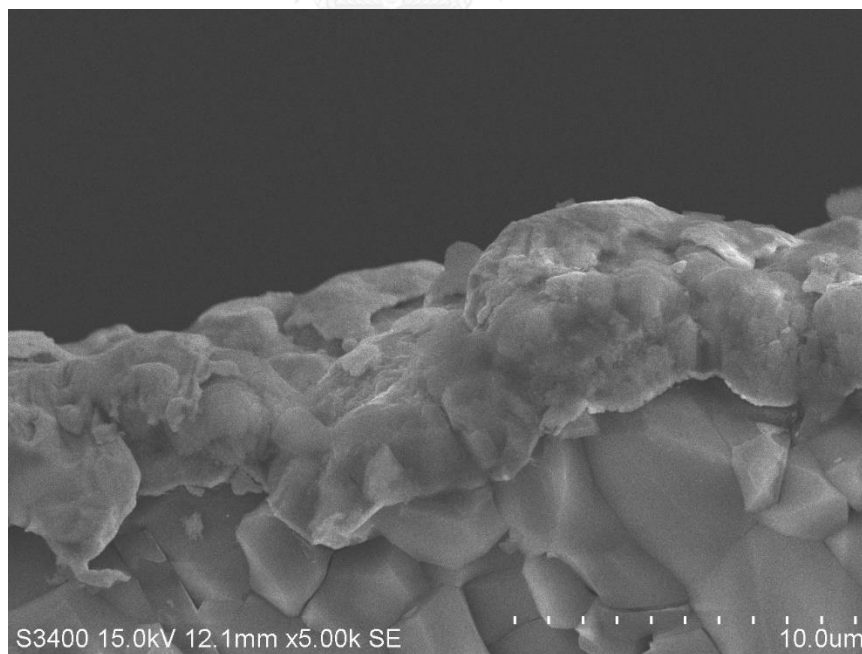

Figure E.6 SEM image of the cross sectional view of YSZ thin film deposited on alumina using conventional method: Au sputter – YSZ(O$_2$) 8 h - Pt

To optimize the performance of the YSZ electrolyte layer at elevated temperatures. When appropriately oxidized, the resulting yttria-stabilized zirconia stoichiometry is $(Y_2O_3)_{0.08}(ZrO_2)_{0.92}$. This 8% yttria composition yields the optimum oxygen-ion conductivity for cubic YSZ. The YSZ sample is characterized using Energy Dispersive X-ray spectroscopy (EDX). The desired concentration of a YSZ film composed of 8% yttria is normally 5 at% Y, 29 at% Zr and 66 at% O.

Table E.1 EDX characterization YSZ(O_2) at 4 h sputtering

Element	Wt%	At%
OK	27.03	67.80
YL	08.45	03.81
ZrL	64.52	28.39
Matrix	Correction	ZAF

Table E.2 EDX characterization YSZ(O_2) at 8 h sputtering

Element	Wt%	At%
OK	29.45	70.33
YL	10.74	04.62
ZrL	59.81	25.05
Matrix	Correction	ZAF

For example, $(Y_2O_3)_{0.08}(ZrO_2)_{0.92}$ = 16 mol% of Y, 92mol% of Zr, 208mol% of O

Summary   = 16+92+208   = 316

Percent of element ; Y = $\dfrac{16}{316} x100 \approx$ 5 at%

Zr = $\dfrac{92}{316} x100 \approx$ 29 at%

O = $\dfrac{208}{316} x100 \approx$ 66 at%

The results of calculation is as good as characterization.

APPENDIX F

THE CHARACTERIZATION CATALYST BY XRD TECHNIQUE

The XRD analysis of YSZ thin film deposited on alumina substrate with different method. By analyzing these XRD patterns, confirmed that all of the samples are well-developed and finely crystalline for conventional method and observed that Au sputter – $YSZ(O_2)$ – Pt led to a more crystalline phase.
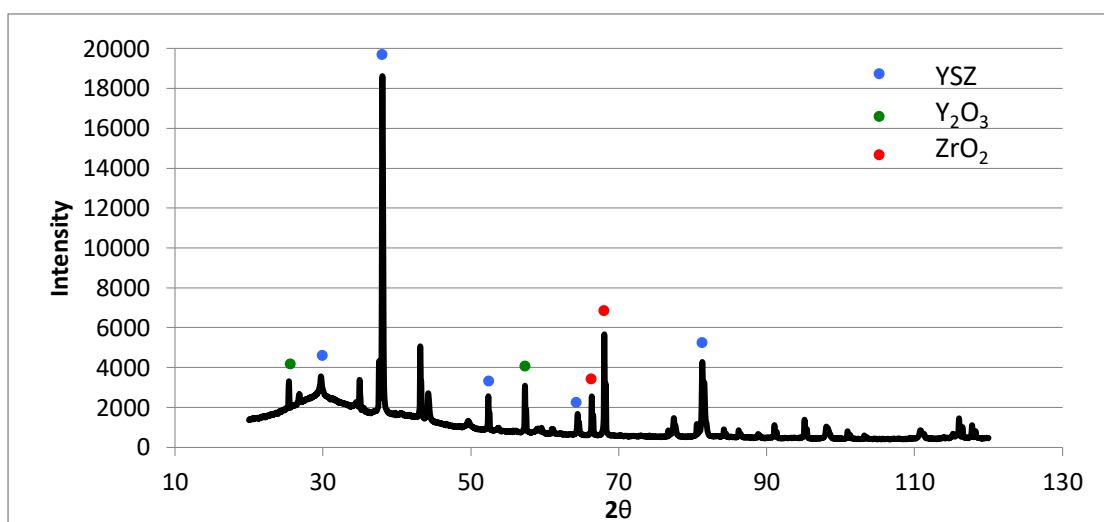

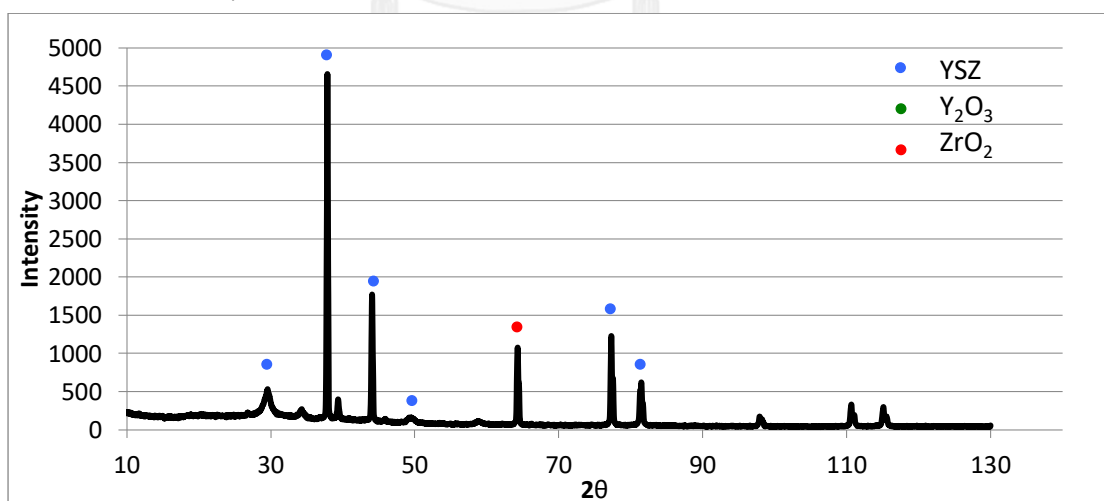**Figure F.1** XRD patterns of YSZ films by wireless method : 200 W for 4 h condition

Figure F.2 XRD patterns of YSZ films by conventional method :
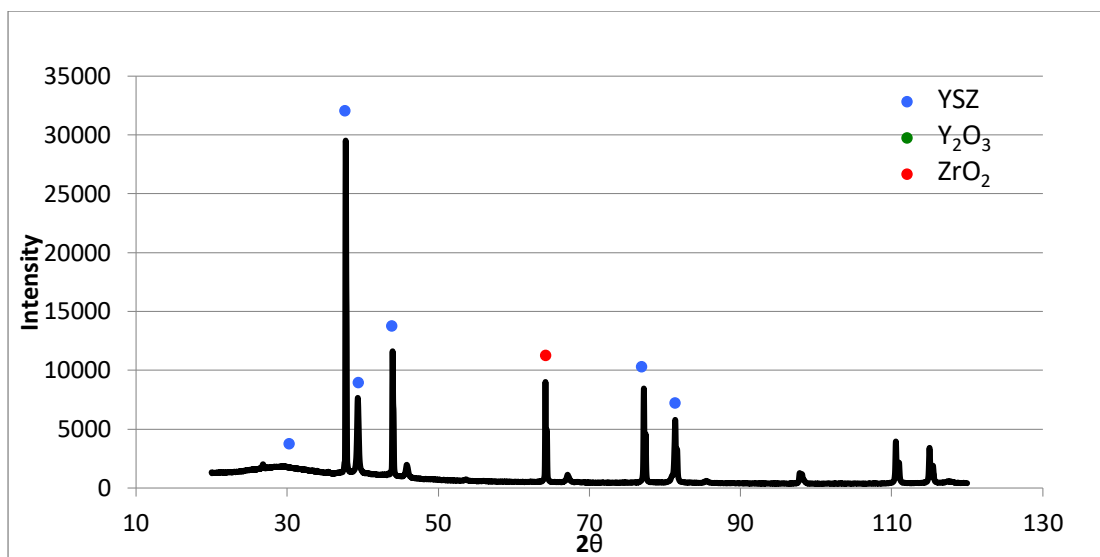
Au paste-YSZ-Pt condition

Figure F.3 XRD patterns of YSZ films by conventional method:
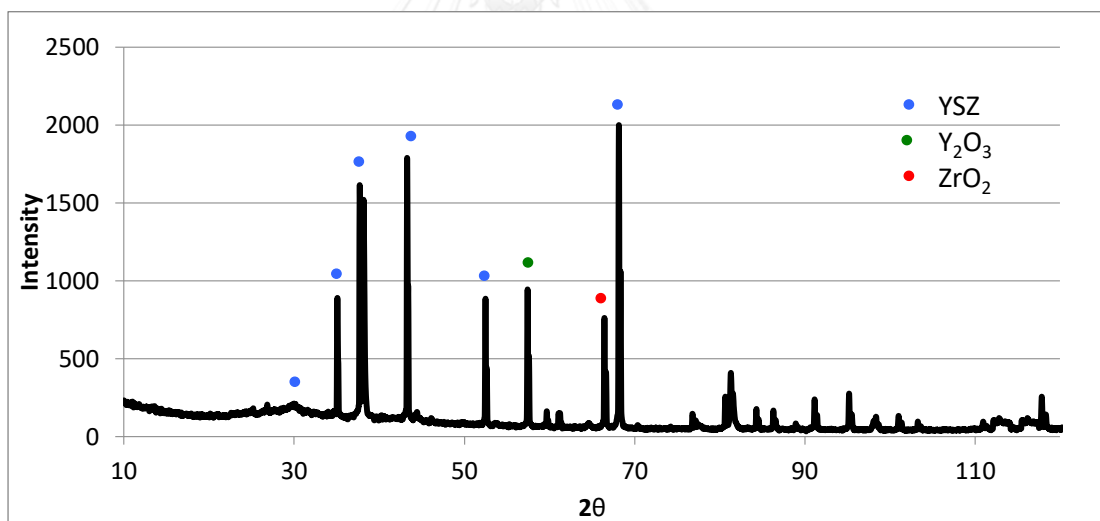
Au paste-YSZ(O₂)-Pt condition

Figure F.4 XRD patterns of YSZ films by conventional method:

Au sputter-YSZ(O₂)-Pt condition

APPENDIX G

IR SPECTROSCOPY AND GAS CHROMATOGRAPHY ANALYSIS

Gas chromatography was used for the gas analysis compared with IR on-line spectroscopy. CO_2 concentration was detected. From IR spectroscopy recorded in %vol of CO_2 . Reactants were standards of C_3H_8 and O_2 in He. The sample was collected amount 1 ml every applying potentials. From accuracy analysis of IR spectroscopy by gas chromatography has not error exceed 20-30% which are acceptable values for these experimental as shown in Table G.1. For example synthesized by conventional method: Au paste - YSZ (O_2) – Pt

Table G.1 Gas chromatography and on-line IR spectroscopy comparison

Au paste-YSZ(O_2)-Pt		CO$_2$				%ERROR
		Gas chromatography		On-line IR spectroscopy		
Temp	Voltage	Area	mol/ml	%vol	mol/ml	
200 °C	Open circuit	973	3.51858E-08	0.117	4.78253E-08	26.43
	0.2 V.	1479	5.34839E-08	0.114	4.6599E-08	14.77
	0.4 V.	1119	4.04655E-08	0.103	4.21026E-08	3.89
	0.6 V.	950	3.43541E-08	0.102	4.16938E-08	17.60
	0.8 V.	785	2.83873E-08	0.096	3.92413E-08	27.66
300 °C	open circuit	3216	1.16298E-07	0.25	1.02191E-07	13.80
	0.5 V.	2563	9.26837E-08	0.228	9.3198E-08	0.55
	1.0 V.	2178	7.87613E-08	0.208	8.50227E-08	7.36
400 °C	open circuit	2745	9.92652E-08	0.238	9.72856E-08	2.03
	0.5 V.	3012	1.08921E-07	0.224	9.1563E-08	18.96
	1.0 V.	2987	1.08016E-07	0.22	8.99279E-08	20.11
500 °C	open circuit	3498	1.26495E-07	0.38	1.5533E-07	18.56
	0.5 V.	4506	1.62947E-07	0.456	1.86396E-07	12.58
	1.0 V.	5971	2.15924E-07	0.489	1.99885E-07	8.02

<u>For example</u>;

- Gas chromatography
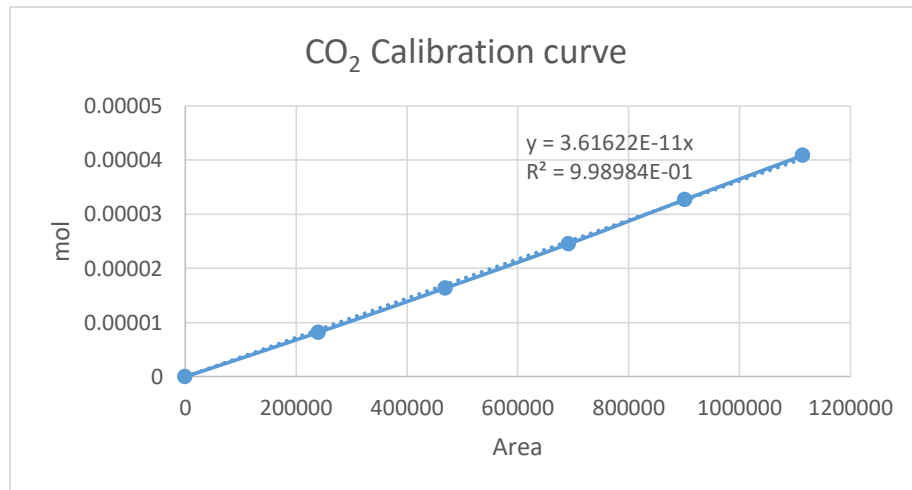
Figure G.1 Calibration curve of CO_2 from Gas chromatography

Peak area CO_2 at 0.4 V ,200 ˚C= 1119 = 1119 x 3.61622 x10^{-11} = 4.04 x10^{-8} mol/ml

- IR-Spectroscopy

IR-recorder at 0.4 V, 200 ˚C = 0.103 %vol

$$= \frac{0.103 \ cm^3 x 1.01325 \ bar}{100 cm^3 x 83.14 \ cm^3 bar \ mol^{-1} K^{-1} x 298.15 \ K}$$

$$= 4.21 x 10^{-8} \ mol/ml$$

Error = $\dfrac{4.21x10^{-8} - 4.04 \ x10^{-8}}{4.21x10^{-8}}$ $x100$ =   3.89 %Error

VITA

Miss Pattamon Limsrimongkonchai

Education : Master of Engineering in Chemical Engineering at Chulalongkorn University, Bangkok, Thailand. Thesis title "Non-faradaic electrochemical modification of catalytic activity (NEMCA) of propane oxidation at thin-film cell on alumina" and Bachelor of Engineering in Chemical Engineering at Mahidol University. Nakhonpathom, Thailand. 2011-2014.

List of publication: Pattamon Limsrimongkonchai and Palang Bumroongsakulsawat, "Non-faradaic electrochemical modification of catalytic activity (NEMCA) of propane oxidation at thin-film cell on alumina", Proceeding of The Pure and Applied Chemistry International Conference 2017, Centra Government Complex Hotel & Convention Centre Chaeng Watthana, Bangkok, Thailand, February 2-3, 2017

จุฬาลงกรณ์มหาวิทยาลัย
CHULALONGKORN UNIVERSITY